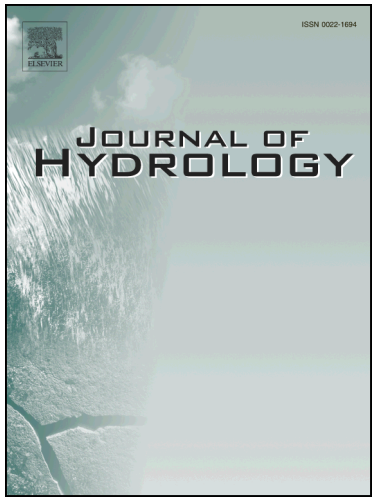

Research papers

To what extent does hydrological connectivity control dynamics of faecal indicator organisms in streams? Initial hypothesis testing using a tracer-aided model

Aaron J. Neill, Doerthe Tetzlaff, Norval J.C. Strachan, Chris Soulsby

PII: S0022-1694(19)30044-7
DOI: https://doi.org/10.1016/j.jhydrol.2018.12.066
Reference: HYDROL 23396

To appear in: *Journal of Hydrology*

Received Date: 15 June 2018
Revised Date: 22 December 2018
Accepted Date: 24 December 2018

Please cite this article as: Neill, A.J., Tetzlaff, D., Strachan, N.J.C., Soulsby, C., To what extent does hydrological connectivity control dynamics of faecal indicator organisms in streams? Initial hypothesis testing using a tracer-aided model, *Journal of Hydrology* (2019), doi: https://doi.org/10.1016/j.jhydrol.2018.12.066

To what extent does hydrological connectivity control dynamics of faecal indicator organisms in streams? Initial hypothesis testing using a tracer-aided model

Aaron J. Neill[a], Doerthe Tetzlaff[a,b,c], Norval J. C. Strachan[d], Chris Soulsby[a]

[a]Northern Rivers Institute, School of Geosciences, St Mary's Building, Elphinstone Road, University of Aberdeen, Aberdeen, AB24 3UF, Scotland, United Kingdom. Emails: aaron.neill@abdn.ac.uk; c.soulsby@abdn.ac.uk

[b]IGB Leibniz Institute of Freshwater Ecology and Inland Fisheries, Berlin, Germany. Email: d.tetzlaff@igb-berlin.de

[c]Department of Geography, Humboldt University Berlin, Berlin, Germany.

[d]School of Biological Sciences, University of Aberdeen, Cruickshank Building, St Machar Drive, Aberdeen, AB24 3UU, Scotland, United Kingdom. Email: n.strachan@abdn.ac.uk

Corresponding Author:

Aaron J. Neill

Northern Rivers Institute, School of Geosciences, St Mary's Building, Elphinstone Road, University of Aberdeen, Aberdeen, AB24 3UF, Scotland, United Kingdom.

Email: aaron.neill@abdn.ac.uk

Abstract

The role of hydrological connectivity in driving the dynamics of faecal indicator organisms (FIOs) in streams is poorly characterised. Here, we demonstrate how a tracer-aided hydrological model can be used within a coupled modelling approach to explore the role of connectivity in governing stream faecal coliform (FC) dynamics. To do so, we tested a hypothesis that in northern upland catchments, the dynamics of hydrological connectivity between major landscape units (hillslopes and riparian zone) and the stream exert a dominant control on stream FC loads by facilitating generation of runoff-driven FC fluxes. This hypothesis was conceptualised within a simple FC model that was coupled to a tracer-aided hydrological model developed for a small (3.2 km^2) data-rich catchment in NE Scotland. The model was dual-calibrated to daily discharge and stable isotope data for the period August 2008 to September 2009; stream FC loads were also simulated but not used as a calibration target. Behavioural models successfully captured the general dynamics of the discharge and isotope data (average Kling-Gupta efficiencies of 0.72 and 0.53, respectively), providing confidence in the realism of simulated hydrological processes. The models simulated a seasonally-varying role of connectivity in driving stream FC loads. In summer, connectivity of the catchment hillslope was crucial in providing a source of FC to the riparian zone for transfer to the stream; this countered the decline in fresh FC input to the riparian zone in summer which reflected the seasonal movement of red deer (the principal source of FC) onto higher ground. In winter when this seasonal movement caused FC to be predominantly stored in the riparian zone, simulated hillslope connectivity primarily provided water to the riparian zone that permitted increased runoff generation and associated mobilisation of FC. Comparison of observed and simulated stream FC loads revealed model performance to be variable (R^2 range: 0-0.34). The better performance of the model in summer was consistent with hydrological connectivity being a dominant control on stream FC loads at this time. However, failure of the model to capture low FC loads in winter indicated that additional processes not considered in the model may also govern stream FC dynamics during this period. Incorporating the impact of freeze-thaw cycles on FC mortality, or a dilution effect of hillslope connectivity in winter, could be potential next steps in refining the hypothesis conceptualised in the FC model presented here. The novel coupled modelling approach used in this study successfully allowed a hypothesised role of connectivity in driving stream FC dynamics to be

tested, contextualised by the accuracy of discharge and isotope-tracer simulations as indicators of hydrological process realism. Therefore, coupling FIO and tracer-aided hydrological models has clear promise for furthering understanding of FIO dynamics, which is a vital precursor to the successful management of microbial water quality. Based on the experiences in this study, a "roadmap" for the future development and application of coupled approaches is also presented.

Key Words: Conceptual models; Faecal coliforms; Flow pathways; Microbial water quality; Stable isotope tracers; Upland catchments

1. Introduction

The extent to which spatio-temporal variations in hydrological connectivity govern the dynamics of faecal indicator organisms (FIOs) in streams represents a key area of research in relation to understanding microbial water quality (Oliver et al., 2016). FIOs, such as faecal coliforms (FC) and generic *E. coli*, are commonly used to indicate faecal contamination of waters, and thus the potential presence of faecal pathogens (Geldreich, 1996). Such pathogens, for example *E. coli* O157, can lead to gastrointestinal illness in humans if exposure occurs via consumption or recreational use of contaminated water (Fewtrell and Kay, 2015; Oliver et al., 2005). Whilst linkages between hydrological connectivity and faecal contamination have begun to receive attention in agricultural landscapes (e.g. Dorner et al., 2006; Muirhead and Monaghan, 2012; Porter et al., 2017), the issue has remained relatively unexplored in upland environments. This is despite a generally greater reliance on poorly-treated private drinking water supplies in such areas (Rodgers et al., 2003) and the role of headwater streams in influencing downstream water quality (Bishop et al., 2008; McDonnell and Beven, 2014).

Catchment-scale numerical models can be used as learning tools to further develop and refine process understanding (Dunn et al., 2008). In particular, testing different process-based model conceptualisations against observational data as competing hypotheses of catchment functioning, and informing future data collection needs through model application, has been advocated within the hydrological community (Beven, 2012; Clark et al., 2011; Gupta and Nearing, 2014). It has also been suggested that process-based models could be similarly used to address fundamental knowledge gaps in relation to the fate and transport of FIOs in catchments (de Brauwere et al., 2014; Oliver et al., 2016). Several such models that simulate both hydrological and FIO dynamics at the catchment scale already exist (e.g. Hipsey et al., 2008; Sadeghi and Arnold, 2002; Whitehead et al., 2016; Wilkinson et al., 2011). However, attempts to capture the many complex and often poorly-understood processes that are thought to affect the fate and transport of FIOs commonly result in highly-parameterised models that can be characterised by large degrees of uncertainty (Cho et al., 2016a; Porter et al., 2017). Furthermore, most existing FIO models only permit the adequacy of hydrological process representation to be

assessed based on how well the model can simulate discharge at the catchment outlet (Cho et al., 2016a). However, discharge data alone cannot be used to assess how well the model represents internal catchment states and processes that strongly drive hydrological connectivity (Birkel et al., 2014; McDonnell and Beven, 2014). These limitations may, therefore, restrict many current FIO models in being used to understand the role of hydrological connectivity in driving stream FIO dynamics (c.f. Kirchner, 2006; Vache and McDonnell, 2006).

One route forward could be to explore modelling approaches that test hypotheses focused on identifying the dominant processes that underlie the complex dynamics often exhibited in catchment-scale empirical observations (Gupta and Nearing, 2014; McDonnell et al., 2007; Sivakumar, 2008). In a hydrological context, this approach has been particularly fruitful when applied in long-term experimental research catchments for which diverse datasets are available to inform process conceptualisation and aid in model testing (Tetzlaff et al., 2017). For example, the collection of long-term stable isotope and geochemical tracer data alongside traditional hydrometric data has allowed for the development of conceptual process-based tracer-aided models, which simultaneously simulate storage-driven water fluxes and their associated tracer concentrations (Birkel and Soulsby, 2015). Such models have led to substantial progress in the characterisation of flow paths, storage dynamics and connectivity for catchments in a wide range of environments, such as northern latitudes (McMillan et al., 2012; Smith et al., 2016; Tunaley et al., 2017), tropical regions (Birkel and Soulsby, 2016; Westerberg and Birkel, 2015) and karst landscapes (Zhang et al., 2017; 2018). This has largely been possible through the "grey box" approach adopted by such models, whereby perceptions of the dominant hydrological processes operating within a catchment are conceptualised within a parsimonious model structure (Birkel and Soulsby, 2015). Models are then evaluated based on their ability to simulate not only observed discharge data, but also to correctly capture the internal states and processes within a catchment that integrate to drive observed tracer dynamics at the catchment scale (Birkel et al., 2015; McDonnell and Beven, 2014). Through adopting a parsimonious approach, it is also possible for such models to be iteratively developed to test refined hypotheses of catchment

functioning as data availability and ideas about dominant processes evolve (Birkel and Soulsby, 2015; Dunn et al., 2008). Similar modelling approaches to test the dominant processes driving the dynamic FIO response of catchments have not yet been fully explored. This is despite it having been suggested that of the many factors thought to influence the fate and transport of FIOs (e.g. release kinetics, entrainment processes, streambed deposition and resuspension, and environmental factors such as pH and salinity affecting die-off [Cho et al., 2016a]), some, such as hydrological processes and temperature, may exert stronger controls (Kay et al., 2007; Tetzlaff et al., 2010; Bluestein et al., 2013).

Conceptual process-based tracer-aided models are not without their limitations. For example, there is a general need for calibration to the specific period of application and a necessary increase in parameterisation to allow for tracer simulation (Birkel and Soulsby, 2015). However, such models still have unrealised potential in providing greater confidence in the realism of simulated catchment hydrological functioning such that linkages between hydrological processes and water quality can be assessed (Birkel and Soulsby, 2015; Hrachowitz et al., 2016). In this work, we present a "proof-of-concept" in this regard with respect to microbial water quality. Specifically, we demonstrate how a tracer-aided model can provide a framework within which the role of hydrological connectivity in governing stream FC dynamics can be explored through a coupled modelling approach. The tracer-aided model employed in this study has been developed for the Bruntland Burn (BB) catchment in NE Scotland. The BB provides an ideal location for this study for two reasons. Firstly, the rich long-term hydrometric and tracer datasets collected for both the stream and spatially-distributed soil and groundwater monitoring locations, have been used to extensively inform and test the tracer-aided model structure (Birkel et al., 2010; 2014a; 2015; Soulsby et al., 2015). This has helped reinforce the consistency of the model with internal catchment processes (Birkel et al., 2014a), which in turn has offered confidence in its use to explore the hydrological drivers of water quality parameters such as dissolved organic carbon (Birkel et al., 2014b; Dick et al., 2015). Secondly, rapid rates of warming and changing precipitation patterns are expected to significantly impact water quantity and quality in northern upland environments such as the BB (Capell et al., 2013; Kundzewicz et al., 2007). Therefore,

understanding the drivers of faecal contamination in such landscapes is critical if future microbial water quality is to be maintained.

To provide the "proof-of-concept", the specific aim of this study was to test a hypothesised role of hydrological connectivity in governing stream FC dynamics. In northern upland catchments, storage-driven connectivity between major landscape units (hillslopes and riparian zone) and the stream has been shown to be a dominant factor in driving the non-linear hydrological response characteristic of such environments (Soulsby et al., 2006; Spence and Woo, 2003; Tetzlaff et al., 2014). As such, we hypothesised that the dynamics of hydrological connectivity between landscape units and the stream also exert a dominant control on stream FC loads by facilitating generation of runoff-driven FC fluxes. Furthermore, we also suggest that groundwater makes a negligible contribution to stream FC, since near-surface and overland flow paths often dominate the hydrological response (Tetzlaff et al., 2010; Tyrell and Quinton, 2003), and that die-off of FC on the land surface is controlled by temperature (Bluestein et al., 2013). We conceptualised this hypothesis of catchment functioning within a simple FC model which we coupled to the tracer-aided hydrological model. The validity of the hypothesis was then tested through addressing the following objectives:

1. Use the model to spatially disaggregate sources and stores of water and FC to examine how hydrological connectivity between landscape units drives the simulated catchment-scale hydrological and FC responses.
2. Assess the performance of the model in simulating observed catchment-scale FC loads, contextualised by the accuracy of discharge and isotope-tracer simulations as indicators of hydrological process realism.

Based on our experience we also use the coupled model as a learning tool to suggest future improvements needed when combining FIO and tracer-aided hydrological models to better capture controls on stream FIO dynamics.

2. Study Site

The study was based at the BB (3.2 km^2), a tributary of the long-term Girnock Burn research site (31 km^2) in the Cairngorms National Park, NE of Scotland. The Girnock is a headwater of the River Dee, which is of great importance for conservation and as a regional drinking-water resource (Langan et al., 1997; Soulsby et al., 2016). The BB has a temperate / boreal oceanic climate. Mean annual air temperature is ~6 ˚C, ranging between 1 ˚C and 12 ˚C in winter and summer, respectively. On average, the BB receives ~1000mm of precipitation per year, which is generally evenly-distributed temporally in low-intensity rainfall events. Annual evapotranspiration averages ~400 mm.

The glacial legacy of the BB causes the catchment to have a wide, flat valley bottom surrounded by steeper hillslopes (Figure 1a). Furthermore, 70% of the catchment is overlain by glacial drift deposits. Previous hydrogeophysical work has indicated that this drift extends to depths of 5-10 m on the steeper hillslopes and up to 40 m in the valley bottom (Soulsby et al., 2016), and acts as a significant store and contributor of groundwater (Birkel et al., 2011b; Blumstock et al., 2015). Soils in the catchment form a classic catena sequence, grading from more freely-draining podzols and rankers on the steeper hillslopes to poorly drained peaty-gleys and peats (up to 4 m deep) in the valley bottom riparian zone (Figure 1b). The riparian zone remains close to saturation throughout the year, with the areal extent of saturation varying between 2% and 40% of total catchment area, depending on antecedent conditions (Figure 1a; Birkel et al., 2010). Saturation-excess overland flow from the riparian zone is the main source of runoff generated in response to precipitation events (Tetzlaff et al., 2014). However, the magnitude of the storm response is highly non-linear, depending strongly on hydrological connectivity between the steeper hillslopes and riparian zone (Soulsby et al., 2015). During wetter periods, expansion of the saturated area facilitates connectivity between these two parts of the catchment via lateral flow to produce the largest responses (Birkel et al., 2015). In drier conditions, however, the hillslopes can become disconnected from the riparian zone due to the predominance of vertical drainage that recharges groundwater (Blumstock et al., 2016; Tetzlaff et al., 2014). In the driest of conditions, baseflow in the stream is largely sustained by groundwater from the underlying drift deposits (Blumstock et al., 2015).

195 The hydrological functioning of the BB has been extensively studied and more details can be found in
196 earlier work (e.g. Geris et al., 2015; Tetzlaff et al., 2014).

197

198 [*Figure 1*]

199

200 In the BB, high densities of red deer (*Cervus elaphus*) provide a key source of faecal contaminants,
201 though contributions from smaller animals such as otters, water voles and mountain hares may also be
202 possible (Tetzlaff et al., 2010). Results from a census of red deer densities in Scotland suggest densities
203 in the BB could be as high as 11-14.9 deer km^{-2} (SNH, 2016), and excreted faecal material from deer is
204 often clearly observable in the catchment. Generally, red deer in Scotland are more likely to occupy
205 higher-elevation areas during summer, coming down into the valley bottoms during winter (Mitchell et
206 al., 1977). However, the detailed movement of red deer is highly complex, varying on a range of
207 timescales in different landscapes in response to various factors (Mitchell et al., 1977).

208

209 **3. Data and Methods**

210 *3.1 Hydrometric, isotope and microbiological data*

211 The study period was 12 August 2008 to 22 September 2009. Stream discharge was derived from stage
212 measurements recorded at 15-minute intervals at the catchment outlet (Figure 1a) using an Odyssey
213 capacitance logger (Odyssey by Dataflow Systems Pty Ltd, New Zealand) and an established rating
214 curve. Meteorological data were primarily based on data collected by an automated weather station 1
215 km away operated by Marine Science Scotland, with daily average temperature being attitudinally
216 corrected. Potential evapotranspiration (PET) was derived from these data using the Penman-Monteith
217 equation (Allen et al., 1998). Catchment precipitation was interpolated using an inverse distance
218 elevation gradient algorithm similar to Capell et al. (2012) based on five surrounding rain gauges

maintained by the Scottish Environmental Protection Agency. All hydrometric data was aggregated into a daily dataset.

ISCO 3700 autosamplers were used to collect stream water spot samples at the catchment outlet (Figure 1a) and bulk precipitation samples at daily intervals for stable isotope analysis. A layer of paraffin was added to bottles used to collect samples for isotope analysis to prevent evaporation. Samples were analysed for deuterium (δ^2H) and oxygen-18 ($\delta^{18}O$) using a Los Gatos DLT-100 laser isotope analyser (precision of ±0.4‰ for δ^2H and 0.1‰ for $\delta^{18}O$). Isotope data are expressed in δ-notation with respect to the Vienna Standard Mean Ocean Water. Given the higher relative precision of δ^2H, these data were used for modelling purposes.

Stream water samples were also collected at approximately weekly intervals for FC analysis. Samples were collected in sterilised bottles, with the standard membrane filtration method using mFC agar plates incubated at 44 ˚C for at least 18 h (APHA, 1992) adopted to determine concentrations of FC, in colony forming units (CFU) 100 ml^{-1}, within 3-4 hours of sample collection. In all cases, an undiluted sample of 100 ml was filtered, with additional dilutions filtered if samples were suspected to be highly contaminated. As such, the limit of detection for FC was 1 CFU 100 ml^{-1} (approximate 95% confidence intervals for colony counts greater than 20 for 100 ml sample: $count \pm 2count^{0.5}$; otherwise see Table 9222:II in APHA, 1992). FC loads (in CFU day^{-1}) were calculated for the catchment outlet by multiplying concentrations by average daily discharges (converted to units of 100 ml day^{-1}). When concentrations were below the limit of detection, an upper limit to the FC load was calculated using a concentration of 1 CFU 100 ml^{-1}.

3.2 Tracer-aided hydrological model

The tracer-aided hydrological model used has been developed for the BB based on extensive empirical and modelling studies (Birkel et al., 2010; 2015; Soulsby et al., 2015). The reader is referred to these papers for details and only a brief overview follows. The model captures the non-linear hydrological response of the BB by conceptualising the hydrological connectivity between three distinct hydrological stores representing the major landscape units (Figure 2a). The dynamic hillslope and dynamic riparian zone broadly represent the more freely-draining podzols of the hillslopes and the saturation-prone peaty soils of the valley bottom, respectively. There is also a groundwater store. The expansion and contraction of the areal extent of saturation is represented by a model input, *dSat*, which is a daily time series generated by an antecedent precipitation index-type algorithm that describes the daily extent of saturation in the catchment (Birkel et al., 2010). The value of *dSat* on any day is used to distribute daily time series of precipitation (P) and PET between the dynamic hillslope (P_{up}, PET_{up}) and riparian zone (P_{sat}, PET_{sat}), which contribute to or deplete the dynamic storages (S_{up} and S_{sat}, both in mm) of each store (Figure 2a).

[*Figure 2*]

To capture storage-driven threshold processes of runoff generation in the BB (Tetzlaff et al., 2014), the dynamic storages of each hydrological source area are permitted to go into deficit; these have to be filled before runoff can be generated (Birkel et al., 2015). The dynamic hillslope can drain into the dynamic riparian zone (flux Q_{up}, in mm day^{-1}) and recharge the groundwater reservoir (flux R, in mm day^{-1}). Both fluxes are linear functions of S_{up} and are controlled by the rate parameters a and r (in day^{-1}), respectively. Flux Q_{sat} (in mm day^{-1}) is a power function of S_{sat} controlled by the rate parameters k (in units of day^{-1}) and α (dimensionless), and conceptualises the non-linear generation of saturation excess overland flow from the riparian zone to the stream. Streamflow (Q_{stream}, in mm day^{-1}) is the sum of Q_{sat} and Q_{low} (in mm day^{-1}), the latter being a groundwater flux that is a linear function of groundwater storage (S_{low}, in mm) controlled by the rate parameter b (in day^{-1}).

The isotopic composition of water in each hydrological store evolves based on the following equation:

$$\frac{d(cS)}{dt} = \sum_j c_{I,j} I_j - \sum_k c_{O,k} O_k \quad \text{(Eq. 1)}$$

where c is the δ^2H composition (‰) of j storage inflows I_j (e.g. P, Q_{up}, R) and k outflows O_k (e.g. Q_{low}, Q_{sat}) causing changes in the storage S of a hydrological store with isotopic composition c. As each store is assumed to be well mixed, the isotopic compositions of any outflow is equal to the composition of the store from which it came. For the isotope transport simulations, the storage S includes both the dynamic storage and an additional mixing volume (MV) that does not contribute to runoff generation (Figure 2a). The MVs are dynamic in time, arising from calibrated storage parameters for each store (upS_p, $lowS_p$, $satS_p$ in mm) that are converted to daily MVs based on the value of *dSat*. In wetter conditions when *dSat* is larger, the expansion of the saturated riparian area causes greater potential for mixing in this part of the catchment at the expense of mixing on the hillslopes (Figure 2a). By dynamically varying the mixing that takes place in the riparian zone and hillslope stores, the complete mixing of the individual storages is integrated at the catchment scale in a non-linear manner, thus resulting in a partial mixing mechanism. The additional mixing volumes are required to capture the importance of large storage volumes that are necessary to damp the isotopic signature of streamflow with respect to precipitation, as shown in previous work (Birkel et al., 2011a; Soulsby et al., 2015).

Previous work in the BB showed that evaporative isotopic fractionation is an important process changing isotopic compositions, particularly in the riparian zone where the fractionated isotopic signal can be translated to stream water (Sprenger et al., 2017). As such, fractionation was accounted for in the dynamic riparian zone of the model using the following equation, based on Benettin et al. (2017, Appendix B):

$$\frac{d[\delta^2 H_{sat}(t)]}{dt} = (1 - \alpha_{ET})\frac{AET_{sat}(t)}{S_{sat}(t) + satMV\ (t)}(\delta^2 H_{sat}(t) + 1000) \quad \text{(Eq. 2)}$$

which conceptualises the change in the isotopic composition of riparian zone storage ($\delta^2 H_{sat}$, in ‰) at time *t* as a function of an isotopic depletion factor (α_{ET}), actual evapotranspiration (AET_{sat}, in mm) from the riparian zone, total storage in the riparian zone (S_{sat} + *satMV*) and the isotopic composition of the riparian zone, at time *t*. The term α_{ET} requires calibration, and can vary between 0 and 1. A value of 1 indicates no fractionation (Benettin et al., 2017). Eq. 2 is used to directly provide an enrichment amount ($frac_{sat}$ in Figure 2a) that is added to the simulated isotopic composition of the riparian zone storage at each timestep to account for evaporative fractionation.

3.3 Faecal coliform model

Since we suggest that FC contributions from groundwater will be negligible, the FC model considers only two stores of FC: the dynamic hillslope and dynamic riparian zone (Figure 2b). To be consistent with trying to adopt a modelling approach that refrains from trying to conceptualise all the complex processes relating to FIOs, we adopt a simple loading function for FC that attempts to capture just the seasonal movements of red deer (assumed to be the major source of FC in the BB). At each time-step, the presence of deer in the catchment is randomly determined. If deer are present, uniform random sampling is used to determine a total number of deer in the catchment between 1 and 50 – the upper limit reflects the upper deer density of 14.9 deer km^{-2} reported for the BB by SNH (2016). A sinusoidal function describing the probability of deer being in the riparian zone is then used to distribute the total number of deer between the hillslope and riparian zone. The function is at its minimum at the beginning of July, and its maximum at the end of December / beginning of January. As such, deer are most likely to be found on the hillslope at the height of summer and in the riparian zone during winter (Mitchell et al., 1977). FC loading by deer to each store is then calculated by multiplying the number of deer by

daily FC excretion per deer. Uniform random sampling is used to determine the FC excreted per deer at each time step to reflect the fact that this is unlikely to be consistent in time and to account for uncertainty in reported excretion of FC by deer (Oliver et al., 2010). To the authors' knowledge, the latter has not been extensively investigated, with only a single value of 5 x 10^8 CFU $deer^{-1}$ day^{-1} for deer in the Lower Mississippi River Basin (Senjem et al., 2002) being found after a literature review. The range from which daily FC excretion was sampled was ± 1 order of magnitude from this value as a reasonable uncertainty bound (Oliver et al., 2010).

Die-off of FC in storage is modelled based on first-order kinetics using Chick's Law (Chick, 1908):

$$C = C_0 e^{-kt} \quad \text{(Eq. 3)}$$

where C is number of bacteria, C_0 is the starting number of bacteria, k is an inactivation rate constant (in units day^{-1}) and t is time since t_0. The inactivation rate constant for FC in storage was calculated as a function of temperature using the following equation based on the Arrhenius equation:

$$k_{deer}(t) = k_0 \theta^{(T(t) - T_0)} \quad \text{(Eq. 4)}$$

where $k_{deer}(t)$ is the inactivation rate constant (in units of day^{-1}) for FC excreted by deer at time t, k_0 is the inactivation rate constant (in units of day^{-1}) at a reference temperature (T_0) set here to 20 ˚C, θ is a temperature sensitivity parameter (dimensionless), and $T(t)$ is air temperature (in units of ˚C) at time t. Since a literature review did not yield specific values of k_0 and θ for FC from red deer, values for *E. coli* excreted by white-tailed deer of 0.175 day^{-1} and 1.007 were used for each parameter, respectively

(Guber et al., 2015). Since the values of k_0 and θ can be highly dependent on the host animal, it is likely that these values will be more representative for red deer than values specifically for FC but from other animal groups (Guber et al., 2015).

Accounting for inputs of FC (which for the riparian zone also includes inputs from the hillslope – see below) and die-off of FC already in storage, the FC available at time *t* for mobilisation from either the dynamic hillslope or riparian zone is described by:

$$FC(t) = FC_{in}(t) + FC(t-1)e^{-k_{deer}(t)} \quad \text{(Eq. 5)}$$

where *FC(t)* is FC in storage (in CFU) at time *t*, $FC_{in}(t)$ is inputs of FC (in CFU) at time *t*, and the final term in the equation is FC in storage (in CFU) at time *(t-1)* subjected to die-off following Chick's Law with a temperature-dependent inactivation rate constant. To conceptualise the mobilisation and transport of FC as a function of runoff generation, fluxes of FC (*upFC_Flux* and *satFC_Flux*, in CFU day^{-1}) are modelled in a similar manner to that of Wilkinson et al. (2011), whereby the proportion of FC stored in either the dynamic hillslope (*upFC*, in CFU) or riparian zone (sa*tFC*, in CFU) stores that is flushed out with runoff is equal to the proportion that the simulated runoff from either store (Q_{up} or Q_{sat}) is of the maximum observed stream discharge for the study period (Figure 2b). This has physical meaning, as the ability of runoff to transport FC will likely depend on its depth and velocity, as this will determine how effectively the flow can entrain and suspend FC that are either free microorganisms or attached to faeces (Tyrell and Quinton, 2003). Fluxes of FC from the hillslope contribute to the FC that is able to be mobilised from the riparian zone, whilst the simulated stream FC load (in CFU day^{-1}) is simply the FC that is flushed from the riparian zone store (Figure 2b). Given the small channel characteristics of the BB and the high velocity of steep upland streams, we do not consider a channel

store of FC, nor is further die-off of FC in the stream water column considered as it is transported to the catchment outlet.

3.4 Model application

The model was applied with a daily time step and was calibrated for the study period. However, data for the preceding three years were used as spin-up to initialise the model. In total, the coupled model had nine parameters, relating to hydrological and tracer simulation, that required calibration. Calibration was achieved by conducing 5,000,000 Monte Carlo simulations with parameter values drawn randomly from uniform distributions with upper and lower bounds informed by previous applications of the tracer-aided model (Table 1; Birkel et al., 2010; 2015). Behavioural parameter sets were identified as those which simultaneously achieved modified Kling-Gupta efficiencies (KGEs) of ≥ 0.7 and ≥ 0.5 for discharge and isotope-tracer simulations, respectively. A lower threshold for isotope simulations was used since it was expected that the model may not be able to capture the complex shorter-timescale variability in the observed data, but instead reflect the more medium- to longer-term trends (e.g. Page et al., 2007). The modified KGE (Kling et al., 2012) is given by:

$$KGE = 1 - \sqrt{(r_{cor} - 1)^2 + (\beta - 1)^2 + (\gamma - 1)^2} \quad \text{(Eq. 6)}$$

where r_{cor} is the correlation coefficient between simulated and observed values, β is the mean of simulated values divided by the mean of observed values (bias ratio) and Υ is the coefficient of variation of simulated values divided by the coefficient of variation of observed values (variability ratio). To better assess the physical realism of the proposed dominant processes driving stream FC conceptualised within the coupled model, observed FC loads were not used as part of model calibration (c.f. Kuppel et al., 2018). However, an R^2 value was calculated to describe the ability of the model to simulate the observed loads. This metric was chosen to focus on the skill of the model in simulating the timing and

variance, rather than the magnitude, of the observed FC loads, since the ability to capture the latter could potentially be impacted by uncertainties in the input data relating to FC simulations. To account for uncertainty in the magnitude of FC loads when stream FC concentrations were below the limit of detection, two sets of R^2 values were calculated assuming for these periods that either 1) all FC loads were zero, or 2) all FC loads were at their upper limit.

[*Table 1*]

Behavioural parameter sets were retained for simulation of stores and fluxes of water and FC within the catchment, as well as of stream discharge, tracer and FC dynamics. To permit spatial disaggregation of sources and stores of water and FC, the median values of simulated outputs from all behavioural models were taken to represent an average simulation. These values were used to assess the contribution made at each model timestep (instantaneous contribution) by inputs of either water or FC from the hillslope to the total store of water or FC in the riparian zone available for either the generation of evapotranspiration and runoff, or FC fluxes to the stream, during that same timestep:

$$Perc_{Hill}(t) = \frac{Flux_{Hill}(t)}{Input_{Rip}(t) + Flux_{Hill}(t) + Storage_{Rip}(t-1)} * 100 \quad \text{(Eq. 7)}$$

Here, $Perc_{Hill}(t)$ is the contribution (in %) that hillslope fluxes of either water or FC generated at time *t*, $Flux_{Hill}(t)$, make to the total store of water or FC available in the riparian zone for hydrological or FC flux generation at time *t*. The total store available is defined as the store of water or FC in the riparian zone at the end of the last timestep, $Storage_{Rip}(t-1)$, plus inputs from the hillslope, as well as any direct inputs (i.e. precipitation or defecated FC) to the riparian zone, $Input_{Rip}(t)$, at time *t*. Die-off at time *t* of FC already stored in the riparian zone at time *t-1* is accounted for prior to application of Eq. 7. The

percentages of total FC in the BB (*upFC* + *satFC*) stored in either the dynamic hillslope or dynamic riparian zone at the end of each timestep after accounting for FC fluxes were also assessed. For simulation of the stream dynamics, the median and 90% spread (5th to 95th percentile) of outputs simulated by the behavioural models were used as an indication of uncertainty arising from variability in parameter values.

4. Results

4.1 Hydroclimatic, isotope and microbiological dynamics

Hydroclimatic conditions during the study period were typical for the region, generally being characterised by low-intensity precipitation events (< 10 mm day^{-1}) that exhibited limited seasonality, and to which discharge often showed a clear response (Figure 3a). The largest precipitation event occurred in February 2009 (65 mm day^{-1}), which also resulted in the highest observed mean daily discharge of 14.24 mm day^{-1}. Periods of more limited precipitation and predominantly baseflow conditions in the stream were observed for April to early May, and during the latter part of September 2009. During winter, mean daily temperatures could fall to -9.7 ˚C, whilst in summer temperatures peaked at 20.7 ˚C (Figure 3b). PET varied seasonally between 0 and 2.6 mm day^{-1} (Figure 3b).

[*Figure 3*]

The δ^2H of stream water was damped compared to precipitation (Figure 3c), with the former ranging between -72.2‰ and -49.2‰ and the latter between -167.2‰ and -2.3‰. This reflects mixing of incoming precipitation with pre-event water stored in the catchment. However, during larger events where there was a clear discharge response, the precipitation δ^2H signal became more apparent in the stream δ^2H signal. Gaps in the stream isotope data between January and March 2009 arose from autosampler failure.

Concentrations of FC varied over three orders of magnitude (Figure 3d). Concentrations exhibited marked seasonality, being highest during summer (maximum of 3.4 $\log_{10}$ CFU 100 ml^{-1} in August 2008). In winter, meanwhile, concentrations could be below the limit of detection for prolonged periods (e.g. two five-week periods between January and March 2009). A clear response of concentrations of FC to discharge was generally not apparent, although higher-discharge events during summer months were generally associated with elevated concentrations. Calculated FC loads displayed similar temporal dynamics to concentrations, with the peak load of 11.2 $\log_{10}$ CFU day^{-1} corresponding to the peak concentration (Figure 3d). When FC concentrations were detectable, FC loads varied over approximately four orders of magnitude. The upper limits calculated for FC loads when concentrations were below the limit of detection did not exceed 7.9 $\log_{10}$ CFU day^{-1}.

4.2 Model calibration

Of the 5,000,000 initial parameter sets, 34,853 satisfied the criteria to be considered behavioural of simultaneously achieving KGEs of ≥ 0.7 and ≥ 0.5 for discharge and isotope-tracer simulations, respectively. The 90% spread (5^{th} to 95^{th} percentile) of behavioural values for each parameter generally extended across much of the respective initial sampling ranges (Table 1). Exceptions were values for the parameters upS_p, $satS_p$, and, to some extent, α. Both upS_p and $satS_p$, in particular, tended to favour values in the lower part of their respective initial sampling ranges. Therefore, for isotope transport simulation, MVs and hence the potential for mixing was, on average, greatest in groundwater and lowest in the riparian zone ($lowS_p > upS_p > satS_p$). The tendency for α to not have behavioural values at the lower end of the initial sampling range, meanwhile, indicated a preference for more non-linear runoff generation from the riparian zone.

4.3 Spatial disaggregation of sources and stores of water and faecal coliforms

To examine how hydrological connectivity between landscape units drives simulated catchment-scale hydrological and FC dynamics, sources and stores of water and FC within the BB were spatially disaggregated (Figure 4). The importance of hydrological connectivity between the dynamic hillslope and riparian zone in the simulation of non-linear discharge responses at the catchment outlet is apparent from Figure 4b. Hillslope connectivity was induced by most precipitation events, suggesting that hillslope storage deficits were generally quite low. When connected, the peak instantaneous contribution of water from the hillslope to the riparian zone for individual periods of connectivity averaged 34%. This average was representative of periods of connectivity throughout the study period – i.e. contributions did not show a clear seasonal dynamic. The overall maximum contribution of 73% occurred in response to the February 2009 precipitation event. During periods of limited rainfall (e.g. April to early May 2009) when the hillslope was disconnected, sufficient water remained in the riparian zone to generate runoff to the stream; however, groundwater was increasingly responsible for sustaining stream discharge (Figure 4b).

[*Figure 4*]

Unlike contributions of water from the hillslope, instantaneous contributions of FC from the hillslope to the riparian zone showed strong seasonality (Figure 4c). The largest contributions of FC from the hillslope were during May to September, with peak contributions for individual connectivity events averaging 40%, and the maximum contribution of 97% occurring in mid-July 2009. By contrast, peak contributions for individual connectivity events during the remaining months averaged only 7%. This seasonality in contributions of FC, but not of water, from the hillslope arose from the clear seasonal pattern in the distribution of FC stored in the catchment between the hillslope and riparian zone (Figure 4d), which reflected the movement of red deer encapsulated within the FC loading function of the model. Throughout the study period, the simulated total FC stored in the BB was quite stable (average of 11.1 $\log_{10}$ CFU), except following flushing of larger amounts of FC during the two largest discharge

491 events in December 2008 and February 2009. However, the percentage of the FC stored in the riparian
492 zone (hillslope) clearly varied between a maximum (minimum) at the beginning of January and a
493 minimum (maximum) at the beginning of July following a generally sinusoidal pattern. Deviations from
494 this pattern arose when connectivity of the hillslope caused FC to be flushed to the riparian zone to
495 increase the share of the total FC stored in the latter.

496

497 The influence of the spatial distribution of stored FC on the ability of the hillslope to contribute FC to
498 the riparian zone meant that hydrological connectivity had a seasonally-varying role in driving
499 simulated stream FC dynamics of the BB. During the months of October to April, connectivity between
500 the hillslope and riparian zone primarily resulted in increases in stream FC load by causing greater
501 amounts of runoff to be generated from the riparian zone which could mobilise the larger amounts of
502 FC stored in this part of the catchment during these months (Figure 4b-d). Patterns of variability in
503 simulated FC loads during this period generally reflected the patterns of variability in the simulated
504 stream discharge. During the months of May to September, however, connectivity of the hillslope also
505 became important in providing FC to the riparian zone that could be used for the generation of FC fluxes
506 to the stream, to counter the general decline in the proportion of the total FC stored in the riparian zone
507 which reflected the movements of red deer. As a result, stream FC loads during this period showed
508 much greater variability than during October to April, with FC loads peaking in response to the hillslope
509 becoming connected to the riparian zone, but then declining rapidly following disconnection as the
510 generation of FC fluxes from the riparian zone to the stream became increasingly supply-limited.

511

512 *4.4 Simulation of discharge, isotope and FC-load dynamics at the catchment scale*

513 In order to test the validity of the hypothesised dominant controls on FC dynamics conceptualised
514 within the coupled model and, thus, also gain some perspective on the likely physical representativeness
515 of the simulated sources and stores of water and FC described in Section 4.3, the ability of the model

to simulate observed catchment-scale FC loads was assessed, contextualised within the performance of the model in relation to simulating observed discharge and isotope-tracer dynamics.

The average and maximum KGEs achieved by the behavioural models for discharge simulations were 0.72 and 0.86, respectively. Event dynamics and magnitudes of observed discharge peaks were generally well-captured by the behavioural models (Figure 5a); however, it was sometimes the case that subtleties in the observed discharge data were not well-simulated by the models. For example, the behavioural models at times under-estimated the flashiness of the discharge response, with the falling limb of some events (e.g. events in September to November 2008 and the February 2009 peak discharge event) simulated to be more prolonged than was observed in reality. In addition, the ability of the models to capture small observed discharge responses was sometimes inconsistent, with the models over-estimating the small discharge response that occurred in mid-October 2008, and under-estimating two small discharge responses that occurred in mid-July 2009. Periods of low flow, such as April to mid-May 2008, also tended to be slightly under-estimated.

Variations in the stream water isotope signal were captured reasonably well, with average and maximum KGEs of 0.53 and 0.62 achieved by the behavioural models, respectively. The models successfully reproduced the damped signal of the stream with respect to precipitation (Figure 5b), and also captured the summer enrichment of the stream isotope signal more successfully than previous applications of the model (e.g. Birkel et al., 2014; Soulsby et al., 2015). The overall skill of the model in simulating the observed isotope signal was probably linked to an extent to the accuracy of discharge simulations. For example, deviations between the observed and simulated isotope signal during September to November 2008 may reflect the limitations of the model in simulating stream discharge during this period. In other instances where discharge simulations were more accurate, deviations between observed and simulated isotopes may have reflected incorrect relative contributions of riparian zone runoff and groundwater to stream discharge. For example, at the end of June 2009, the behavioural

542 models simulated isotope values that were too enriched relative to observations, which may reflect the
543 models translating too much of the enriched precipitation signal at that time (Figure 3c) to the stream
544 via riparian zone runoff, at the expense of contributions of groundwater that typically has a more
545 depleted isotopic composition (Soulsby et al., 2015). It should be noted, however, that deviations
546 between observed and modelled stream isotopes were only on the order of a few per mille, with the
547 general directions of variability in the observed isotope dataset being captured quite well.

548

549 [*Figure 5*]

550

551 The ability of the behavioural models to simulate observed FC loads was variable (Figure 5c), with
552 values of R^2 ranging from 0 to 0.34 across both sets of calculated values. Model performance was best
553 in the summer months, with uncertainty bounds (arising from uncertainty in the tracer-aided
554 hydrological component of the model and the random component of the FC loading function)
555 encompassing some observed FC loads, and also capturing some of the observed dynamics. The main
556 failure of the behavioural models was their inability to capture the seasonality of observed FC loads
557 (Figure 3d). The key period of model failure was January to March 2009. Here, simulated FC loads
558 consistently exceeded the upper limits for observed loads that were calculated for the prolonged periods
559 when FC concentrations were below the limit of detection. Some of the more minor deviations between
560 observed and simulated FC loads probably reflected limitations in the tracer-aided component of the
561 model in capturing some of the subtleties in the observed discharge and isotope data highlighted
562 previously. For example, the over-estimation of FC loads in the latter part of 2008 was likely to have
563 arisen from discharge often being over-estimated in this period, whilst the under-estimation of FC loads
564 in July 2009 may be a consequence of the models not simulating the small discharge events that were
565 observed. In addition, the failure of the models to capture isolated occurrences of lower FC loads may
566 reflect simulation of runoff generation from the riparian zone to the stream when in actuality
567 groundwater was the main contributor to discharge (e.g. at the end of June 2009).

5. Discussion

5.1 Exploring the role of hydrological connectivity in driving catchment-scale FC dynamics with a coupled tracer-aided model

Many process-based FIO models can be impacted by high degrees of parametrisation and uncertainty, and model structures that limit assessment of hydrological process realism and internal catchment states (Cho et al., 2016a; Hrachowitz et al., 2016). This hinders their application in exploring hypotheses that could address fundamental knowledge gaps surrounding the fate and transport of FIOs, including the role that hydrological connectivity plays in governing stream FIO dynamics. (Oliver et al., 2016). Here, the novel coupling of a parsimonious tracer-aided hydrological model and simple FC model has allowed a hypothesised role of hydrological connectivity in governing stream FC dynamics to be tested within the context of the inferred realism of simulated hydrological processes and internal catchment states.

The skill of the hydrological component of the model in simulating the general dynamics of both the observed discharge and tracer responses of the BB (Figure 5a-b) gives reassurance that the hydrological functioning of the catchment is being captured with reasonable accuracy such that the hypothesised role of connectivity in driving stream FC dynamics can be assessed (c.f. McDonnell and Beven, 2014; Vache and McDonnell, 2006). The performance of the coupled model in simulating observed FC loads strongly suggests that hydrological connectivity between landscape units and the stream exhibits an important control on stream FC dynamics through facilitating runoff-driven FC fluxes, at least during certain times of the year (Figure 5c). In particular, an important inference from the modelling was the crucial role of hillslope connectivity in providing FC to the riparian zone during the summer months (Figure 4c-d). When connectivity was established, elevated stream FC loads were simulated that opposed the general decreasing trend in simulated loads over the summer, reflecting the seasonal movement of red deer to the hillslope and the associated reduction of FC stored in the riparian zone (Figure 4d). This allowed some observed FC loads during this period to be bracketed by simulations (Figure 5c), and suggests

that, during the summer months at least, hydrological connectivity between the hillslope and riparian zone can drive non-linearities in stream FC load dynamics. This would be consistent with the importance of connectivity between the hillslope and the riparian zone in driving non-linearities in the hydrological response of northern upland catchments (Figure 4b; Birkel et al., 2015; Tetzlaff et al., 2014; Wells et al., 2017), and in other water quality parameters such as dissolved organic carbon (e.g. Dick et al., 2015).

The failure of the model to capture the seasonality in observed FC loads, however, indicates that the current hypotheses of system functioning conceptualised within the model are insufficient to fully identify the dominant processes driving stream FC dynamics in the BB (c.f. Beven, 2012; Dunn et al., 2008). Since the model continued to capture the general dynamics of the observed discharge and tracer data during the winter (Figures 5a-b), the failure in simulating observed FC loads during this period suggests that it is the hypothesis relating to the processes governing FC production and distribution in the catchment, rather than hydrological functioning, that needs refinement. This is further supported by the wealth of data on which the tracer-aided component of the model is based and its past successes in simulating biogeochemical parameters such as dissolved organic carbon which have a less-complex seasonal dynamic (Birkel et al., 2014a; 2014b; Dick et al., 2015). It is important to note that, to some extent, the well-known need for improved estimates of FIO die-off and loading parameters for wild animals and the resultant uncertainty in the values of these parameters used for red deer in this study are likely to have impacted on FC simulations (c.f. de Brauwere et al., 2014; Guber et al., 2015; Oliver et al., 2016). However, given that the period of significant model failure is restricted to the winter months, it is likely that the hypothesis conceptualised in the FC component of the model may be missing dominant processes affecting FC dynamics during this period.

If it is correct that connectivity exerts a major control on stream FC dynamics through facilitating runoff-driven FC fluxes, the period of model failure would suggest the absence of a process that reduces

620 the store of FC available for transfer to the stream in winter, instead of it remaining fairly stable (Figure
621 4d). Substantial increases in bacteria mortality can occur in response to repeated freeze-thaw cycles
622 (Habteselassie et al., 2008; Natvig et al., 2002). Given the climate in northern upland environments like
623 the BB (Figure 3b), freeze-thaw cycles over winter are common. Dawson et al. (2011) identified that
624 the 42-day antecedent mean temperature is a useful predictor for defining the switchover between
625 summer/autumn and winter/spring biological processes in NE Scotland. If a value for this variable of 2
626 ˚C or less is taken as indicative of when diurnal temperature fluctuations may have allowed freeze-thaw
627 cycles to occur, it can be shown that a substantial part of the key period of model failure between
628 January and March 2009 may have been impacted by increased FC mortality (blue shaded area in Figure
629 5c). As such, one potential refinement to the hypothesis conceptualised within the FC component of the
630 model could be to allow for increased FC mortality in response to repeated freeze-thaw cycles, to
631 determine whether this would permit more successful simulation of winter FC loads. To achieve this,
632 however, would also require efforts to better characterise the non-linearities in inactivation rate
633 constants caused by processes such as freeze-thaw, especially with respect to FIOs from wild animals
634 (c.f. Crane and Moore, 1986; Guber et al, 2015).

635

636 It may also be necessary, however, to consider alternative roles of connectivity in winter to enable the
637 model to capture the lower FC loads. One possibility could be to investigate whether higher influxes of
638 less-contaminated hillslope water dilute FC concentrations in the riparian zone, leading to lower
639 concentrations and loads being observed in the stream. Such a mechanism would be consistent with the
640 riparian zone often being identified as a critical mixing zone which integrates the characteristics of
641 different source waters in a catchment to set stream water quality (Seibert et al., 2009; Tetzlaff et al.,
642 2014; Tunaley et al., 2016). In summer, a riparian dilution effect on more-contaminated influxes of
643 water from the hillslope would be expected to be less pronounced, as a store of FC is maintained in the
644 riparian zone even in the absence of fresh inputs from red deer due to influxes of FC from the hillslope.
645 Testing this new conceptualisation of connectivity would require the model to be modified to deal with

concentrations of FC as well as loads so that increased runoff generation could lead to dilution as well as greater mobilisation of FC.

In addition to the most notable poor performance of the model in winter, there were also other deviations between observed and simulated FC loads, such as in late 2008 and July 2009 (Figure 5c). These may reflect uncertainties in the parameters relating to FC die-off and loading discussed previously, or the need for additional factors to be incrementally incorporated into the FC model to determine whether this allows for more nuanced simulation of FC loads. For example, a channel store where FC can be deposited, subjected to die-off and then re-suspended (e.g. Wilkinson et al., 2011) may contribute to reducing the over-estimation of FC loads in late 2008, whilst allowing for regrowth of FC in warmer temperatures (e.g. Cho et al., 2016b) may increase simulated FC loads in July 2009. As highlighted in Section 4.4, however, it is probable that many of these deviations are simply related to instances when the tracer-aided hydrological component of the model failed to capture subtleties in the observed discharge and isotope data (Figure 5). This was likely a consequence of the lumped structure of the semi-distributed model not being able to capture the drivers of subtle non-linearities in the discharge response of the BB, such as the influence of micro-topography (e.g. Frei et al, 2010) and fill-and-spill mechanisms which establish transient connectivity between the stream and interconnected pools that often make up riparian peatland drainage networks (Lessels et al., 2016; Soulsby et al., 2015; Sprenger et al., 2017). The use of more spatially-distributed models would help overcome these issues, as well as enable sources of FC to be modelled as highly localised phenomena (e.g. individual deer faeces) whose connection to the stream will depend on the spatial distribution of active flow paths (c.f. Dymond et al., 2016).

5.2 Future prospects for combining FIO and tracer-aided hydrological modelling approaches

A prerequisite to using models in exploring hydrological controls on water quality is the realistic simulation of hydrological processes and internal catchment states to which water quality parameters

672 are sensitive (Vache and McDonnell, 2006). In this study, insight into hydrological process realism
673 provided by the tracer-aided model component helped understand whether discrepancies between
674 simulated and observed FC dynamics were indicative of a need to refine the hypothesis conceptualised
675 within the FC component of the model, or if they may have arisen due to inadequacies in the simulation
676 of hydrological processes. In this way, coupling of FIO and tracer-aided hydrological models clearly
677 has promise for assessing how factors such as hydrological connectivity drive stream FIO dynamics.
678 Here, we provide a "roadmap" for the future development and application of coupled FIO and tracer-
679 aided models based on our experiences in this study.

680

681 Integration of stable isotope tracers into spatially-distributed models has been steadily increasing (e.g.
682 Kuppel et al, 2018; Remondi et al., 2018; Stadnyk et al., 2013; van Huijgevoort et al., 2016). Such
683 modelling approaches have been successful in capturing the spatial and temporal dynamics of discharge
684 and stable isotope tracers, and also permit more specific interrogation of how different parts of the
685 catchment contribute to runoff generation under varying hydrological conditions (Ala-aho et al., 2017;
686 Kuppel et al., 2018; Remondi et al., 2018). In this way, such modelling approaches could help overcome
687 some of the structural limitations of the model presented here. Furthermore, spatially-distributed
688 modelling frameworks could also facilitate inclusion of particle-tracking (e.g. Davies et al., 2011) or
689 agent-based strategies (e.g. Reaney, 2008) that can explicitly track water particles and their associated
690 tracer and contaminant characteristics through catchments (Davies et al., 2013). There is potential for
691 developing spatially-distributed modelling with isotopes, particularly with cheaper isotope analysis
692 increasing the viability of conducting repeat synoptic sampling of tracers (e.g. Ala-aho et al., 2018;
693 Lessels et al., 2016) that can be used in calibration or to test how well a model can simulate spatial
694 variability in hydrological processes and tracer concentrations (Birkel and Soulsby, 2015). If combined
695 with efforts to better characterise the spatial distribution of FIO inputs (e.g. with repeated field mapping
696 or use of remote monitoring techniques such as cameras or GPS tags on animals), and synoptic surveys
697 of stream FIO concentrations (which may be feasible using rapid enumeration techniques such as the
698 IDEXX Coliert-18 method, which require very little sample processing time prior to incubation

699 [Kinzelman et al., 2005]), the coupling of FIO models to spatially-distributed tracer-aided models would
700 likely be transformational in elucidating the role of connectivity in driving stream FIO dynamics.

701

702 An important comment relates to data. For the application of spatially-distributed coupled models, the
703 collection of spatially-distributed data relating to FIO loading of the landscape and stream FIO
704 concentrations will be necessary. However, more fundamental requirements for any FIO modelling
705 exercise will, firstly, be the collection of data that can allow more certain characterisation of FIO
706 loadings by wild animals and the associated die-off behaviour of such FIOs (Guber et al, 2015;
707 Muirhead et al., 2011), particularly in relation to extreme conditions such as repeated freeze-thaw cycles
708 experienced over winter. Secondly, there is also a need for means of collecting higher-temporal
709 resolution stream FIO data to be developed. Whilst the weekly data used in this study are informative,
710 data that can resolve shorter-timescale variability in FIO dynamics will help to fully decipher how
711 hydrological processes and microbial water quality are linked (c.f. Kirchner et al., 2004). Standard time
712 frames for the analysis of water samples for FIOs have dictated that the collection of longer-term, high-
713 temporal resolution FIO data has so far only really been possible with intensive field campaigns that
714 involve the collection and processing of grab samples on a daily basis (e.g. Kim et al., 2017). However,
715 with sufficient site-specific investigations on the impact of sample storage time on FIO concentrations,
716 the use of autosamplers may help to ease the logistical burden of collecting longer-term, high-frequency
717 FIO datasets (e.g. Hathaway et al., 2014; Oliver et al., 2015). In addition, there are also emerging
718 technologies that can monitor beta-D-glucuronidase enzymatic activity in streams in near real-time,
719 which may have potential to provide high temporal-resolution data relating to microbial contamination
720 that can complement more traditional means of FIO enumeration (Stadler et al., 2016; Ender et al.,
721 2017). Exploiting these advances in the collection of higher frequency data is likely to be instrumental
722 in permitting a more thorough evaluation of hypothesised linkages between hydrological connectivity
723 and FIO dynamics (de Brauwere et al., 2014; Oliver et al., 2016).

724

Finally, whilst this study has been based at a well-researched, data-rich, temperate site, it should be noted that future applications of coupled FIO and tracer-aided models need not be limited to such locations. For example, previous studies in more data-sparse tropical and karst regions have successfully used shorter-term or event-based tracer data to test and constrain multiple model structures as competing hypotheses of catchment hydrological functioning, despite the potentially greater complexity of hydrological processes operating in such landscapes (Birkel and Soulsby, 2016; Westerberg and Birkel, 2015; Zhang et al., 2017; 2018). As such, there is clear scope for employing coupled modelling approaches in such regions to explore controls on FIO dynamics; indeed, improved FIO modelling approaches in karst systems has been identified as a key research priority, in particular (Buckerfield et al., 2019). In addition, whilst data-rich catchments offer an obvious test-bed for developing new modelling approaches (Tetzlaff et al., 2017), the process understanding gained especially through the application of parsimonious models is likely to be somewhat transferable to similar catchments that have less data availability or are ungauged (c.f. McDonnell et al., 2007). Therefore, insights from parsimonious coupled modelling approaches into the controls on FIO dynamics in data-rich catchments are likely to still be informative for the management of microbial water quality more generally.

Conclusions

In this study, we have provided a "proof-of-concept" with respect to how tracer-aided hydrological models can be used to explore linkages between hydrological processes and microbial water quality. Specifically, we used a simple FC model coupled to a tracer-aided model to assess the hypothesis that hydrological connectivity between landscape units and the stream in northern upland catchments exerts a dominant control on stream FC dynamics by facilitating runoff-driven FC fluxes. The skill of the tracer-aided model component in simulating the general dynamics of observed discharge and isotope data provided confidence in the realism of the hydrological processes simulated by the model. As such, the ability of the model to simulate weekly observed FC loads at certain times of the year inferred that hydrological connectivity is likely a dominant control on stream FC dynamics during these periods. In

752 particular, the crucial role of hillslope connectivity to the riparian zone during summer to provide FC
753 for mobilisation to the stream despite reduced fresh inputs from red deer due to seasonal movements,
754 was highlighted. Failure of the model to simulate lower winter FC loads could have reflected limitations
755 in the data available for driving the FC component of the model. However, the specific timing of model
756 failure more likely indicated a need to refine the hypothesis conceptualised within the FC model,
757 potentially to incorporate the impact of freeze-thaw cycles on FC mortality or a dilution effect of
758 hillslope connectivity in winter. Other deviations between observed and simulated FC loads could
759 highlight the need for additional processes to be incrementally incorporated into the FC model to assess
760 whether they allow for more nuanced simulation of FC loads, but most probably reflected limitations
761 arising from the lumped structure of the model.

762

763 The greater potential for evaluating hydrological process consistency afforded by the use of a tracer-
764 aided model was valuable in assessing whether refinements to the hypothesis conceptualised within the
765 FC model component may be necessary for more successful simulation of observed FC data, or if
766 inadequate hydrological process representation may have resulted in deviations between observations
767 and simulations. As such, coupling FIO and tracer-aided hydrological models has great potential in
768 better understanding the drivers of stream FIO dynamics, particularly if models are applied to test
769 hypotheses which are refined based on model successes and failures, and as new data become available.
770 This will likely have significant value for the effective management of microbial water quality in a
771 range of environments, especially if some of the opportunities for model development and data
772 collection highlighted from our experiences in this study can be realised.

773

774 **Acknowledgments**

775 Funding from the Scottish Government Hydro Nation Scholars Programme is gratefully acknowledged. Many
776 thanks to Mark Speed and Audrey Innes for collecting and analysing the samples from 2008/9, as part of work

777 funded by the Levrhulme Trust. Thanks also to Christian Birkel for discussions in relation to the tracer-aided
778 hydrological component of the model. Please contact the authors for access to the data used in this paper.

779

780 **Declarations of Interest:** None

781

782

783 **References**

784

785 Ala-aho, P., Tetzlaff, D., McNamara, J.P., Laudon, H., Soulsby, C., 2017. Using isotopes to constrain water flux
786 and age estimates in snow-influenced catchments using the STARR (Spatially distributed Tracer-Aided Rainfall-
787 Runoff) model. Hydrological Earth Systems Science 21, 5089-5110.

788

789 Ala-Aho, P., Soulsby, C., Pokrovsky, O.S., Kirpotin, S.N., Karlsson, J., Serikova, S., Vorobyev, S.N., Manasypov,
790 R.M., Loiko, S., Tetzlaff, D., 2018. Using stable isotopes to assess surface water source dynamics and
791 hydrological connectivity in a high-latitude wetland and permafrost influenced landscape. Journal of Hydrology
792 556, 279-293.

793

794 Allen, R.G., Pereira, L.S., Raes, D., 1998. Crop evapotranspiration: guidelines for computing crop water
795 requirements, FAO irrigation and drainage papers 56. FAO, Rome.

796

797 APHA, 1992. Standard Methods for the Evaluation of Water and Wastewater, 18th Edition. American Public
798 Health Association, Washington, DC.

799

800 Benettin, P., Soulsby, C., Birkel, C., Tetzlaff, D., Botter, G., Rinaldo, A., 2017. Using SAS functions and high-
801 resolution isotope data to unravel travel time distributions in headwater catchments. Water Resources Research.
802 53, 1864-1878.

803

804 Beven, K., 2006. A manifesto for the equifinality thesis. Journal of Hydrology 320, 18-36.

805

806 Beven, K., 2012. Causal models as multiple working hypotheses about environmental processes. Comptes Rendus
807 Geoscience 344, 77-88.

808

809 Birkel, C., Soulsby, C., 2015. Advancing tracer-aided rainfall-runoff modelling: a review of progress, problems
810 and unrealised potential. Hydrological Processes 29, 5227-5240.

811

812 Birkel, C., Soulsby, C., 2016. Linking tracers, water age and conceptual models to identify dominant runoff
813 processes in a sparsely monitored humid tropical catchment. Hydrological Processes 30, 4477-4493.
814
815 Birkel, C., Soulsby, C., Tetzlaff, D., 2011a. Modelling catchment-scale water storage dynamics: reconciling
816 dynamic storage with tracer-inferred passive storage. Hydrological Processes 25, 3924-3936.
817
818 Birkel, C., Soulsby, C., Tetzlaff, D., 2014a. Developing a consistent process-based conceptualization of catchment
819 functioning using measurements of internal state varaibles. Water Resources Research 50.
820
821 Birkel, C., Soulsby, C., Tetzlaff., D. 2014b. Integrating parsimonious models of hydrological connectivity and
822 soil biogeochemistry to simulate stream DOC dynamics. Journal of Geophysical Research 119, 1030-1047.
823
824 Birkel, C., Soulsby, C., Tetzlaff, D., 2015. Conceptual modelling to assess how the interplay of hydrological
825 connectivity, catchment storage and tracer dynamics controls nonstationary water age estimates. Hydrological
826 Processes 29, 2956-2969.
827
828 Birkel, C., Tetzlaff, D., Dunn, S.M., Soulsby, C., 2010. Towards a simple dynamic process conceptualization in
829 rainfall-runoff models using multi-criteria calibration and tracers in temperate, upland catchments. Hydrological
830 Processes 24, 260-275.
831
832 Birkel, C., Tetzlaff, D., Dunn, S.M., Soulsby, C., 2011b. Using time domain and geographic source tracers to
833 conceptualize streamflow generation processes in lumped rainfall-runoff models. Water Resources Research 47,
834 W02515.
835
836 Bishop, K., Buffam, I., Erlandsson, M., Fölster, J., Laudon, H., Seibert, J., Temnerud, J., 2008. *Aqua Incognita*:
837 the unknown headwaters. Hydrological Processes 22, 1239-1242.
838
839 Blaustein, R.A., Pachepsky, Y., Hill, R.L., Shelton, D.R., Whelan, G., 2013. *Escherichia coli* survival in waters:
840 Temperature dependence. Water Research 47(2), 569-578
841

Blumstock, M., Tetzlaff, D., Malcolm, I.A., Nuetzmann, G., Soulsby, C., 2015. Baseflow dynamics: Multi-tracer surveys to assess variable groundwater contributions to montane streams under low flows. Journal of Hydrology 527, 1021-1033.

Blumstock, M., Tetzlaff, D., Dick, J.J., Nuetzmann, G., Soulsby, C., 2016. Spatial organisation of groundwater dynamics and streamflow response from different hydropedological units in a montane catchment. Hydrological Processes 30, 3735-3753.

Buckerfield, S.J., Waldron, S., Quilliam, R.S., Naylor, L.A., Li, S., Oliver, D.M., 2019. How can we improve understanding of faecal indicator dynamics in karst systems under changing climatic, population, and land use stressors? – Research opportunities in SW China. Science of the Total Environment 646, 438-447.

Capell, R., Tetzlaff, D., Soulsby, C., 2012. Can time domain and source area tracers reduce uncertainty in rainfall-runoff models in larger heterogeneous catchments? Water Resource Research 48, W09544.

Capell, R., Tetzlaff, D., Soulsby, C., 2013. Will catchment characteristics moderate the projected effects of climate change on flow regimes in the Scottish Highlands? Hydrological Processes 27, 687-699.

Chick, H., 1908. Investigation of the laws of disinfection. Journal of Hygiene 8, 655.

Cho, K.H., Pachepsky, Y.A., Oliver, D.M., Muirhead, R.W., Park, Y., Quilliam, R.S., Shelton, D.R., 2016a. Modeling fate and transport of fecally-derived microorganisms at the watershed scale: State of the science and future opportunities. Water Research 100, 38-56.

Cho, K.H., Pachepsky, Y.A., Kim, M., Pyo, J.C., Park, M.H., Kim, Y.M., Kim, J.W., Kim, J.H., 2016b. Modeling seasonal variability of fecal coliform in natural surface waters using the modified SWAT. Journal of Hydrology 535, 377-385.

Clark, M.P., Kavetski, D., Fenicia, F., 2011. Pursuing the method of multiple working hypotheses for hydrological modeling. Water Resources Research 47, W09301.

Crane, S.R., Moore, J.A., 1986. Modelling Enteric Bacterial Die-off: A Review. Water, Air and Soil Pollution 27, 411-439.

Davies, J., Beven, K., Nyberg, L., Rodhe, A., 2011. A discrete particle representation of hillslope hydrology: hypothesis testing in reproducing a tracer experiment at Gårdsjön, Sweden. Hydrological Processes 25, 3602-3612.

Davies, J., Beven, K., Rodhe, A, Nyberg, L., Bishop, K., 2013. Integrated modeling of flow and residence times at the catchment scale with multiple interacting pathways. Water Resources Research 49, 4738-4750.

de Brauwere, A., Ouattara, N.K., Servais, P., 2014. Modeling fecal indicator bacteria concentrations in natural surface waters: A review. Critical Reviews in Environmental Science and Technology 44, 2380-2453.

Dick, J.J., Tetzlaff, D., Birkel, C., Soulsby, C., 2015. Modelling landscape controls on dissolved organic carbon sources and fluxes to streams. Biogeochemistry 122, 361-374.

Dorner, S.M., Anderson, W.B., Slawson, R.M., Kouwen, N., Huck, P.M., 2006. Hydrologic modeling of pathogen fate and transport. Environmental Science and Technology 40, 4746-4753.

Dunn, S.M., Freer, J., Weiler, M., Kirkby, M.J., Seibert, J., Quinn, P.F., Lischeid, G., Tetzlaff, D., Soulsby, C., 2008. Conceptualization in catchment modelling: simply learning? Hydrological Processes 22, 2389-2393.

Dymond, J.R., Serezat, D., Ausseil, A.G.E., Muirhead, R.W., 2016. Mapping of Escherichia coli sources connected to waterways in the Ruamahanga catchment, New Zealand. Environmental Science and Technology 50(4), 1897-1905.

Ender, A., Goeppert, N., Grimmeisen, F. and Goldscheider, N., 2017. Evaluation of β-d-glucuronidase and particle-size distribution for microbiological water quality monitoring in Northern Vietnam. Science of the Total Environment 580, 996-1006.

902

903 Fewtrell, L., Kay, D. 2015. Recreational water and infection: a review of recent findings. Current environmental
904 health reports 2(1), 85-94.

905

906 Frei, S., Lischeid, G., Fleckenstein, J.H., 2010. Effects of micro-topography on surface–subsurface exchange and
907 runoff generation in a virtual riparian wetland – A modeling study. Advances in Water Resources 13(11), 1388–
908 1401.

909

910 Geldreich, E.E., 1996. Pathogenic agents in freshwater resources. Hydrological Processes 10, 315-333.

911

912 Geris, J., Tetzlaff, D., McDonnell, J., Soulsby, C., 2015. The relative role of soil type and tree cover on water
913 storage and transmission in northern headwater catchments. Hydrological Processes 29, 1844–1860.

914

915 Guber, A.K., Fry, J., Ives, R.L., Rose, J.B., 2015. *Escherichia coli* Survival in, and release from, White-Tailed
916 Deer feces. Applied and Environmental Microbiology 81, 1168-1176.

917

918 Gupta, H.V., Nearing, G.S., 2014. Debates – The future of hydrological sciences: A (common) path forward?
919 Using models and data to learn: A systems theoretic perspective on the future of hydrological science. Water
920 Resources Research 50, 5351-5359.

921

922 Habteselassie, M., Bischoff, M., Blume, E., Applegate, B., Reuhs, B., Brouder, S., Turco, R.F., 2008.
923 Environmental controls on the fate of *Escherichia coli* in soil. Water, Air and Soil Pollution 190, 143-155.

924

925 Hathaway, J.M., Hunt, W.F., Guest, R.M., McCarthy, D.T., 2014. Residual indicator bacteria in autosampler
926 tubing: a field and laboratory assessment. Water Science and Technology 69(5), 1120-1126.

927

928 Hipsey, M.R., Antenucci, J.P., Brookes, J.D., 2008. A generic, process-based model of microbial pollution in
929 aquatic systems. Water Resources Research 44, W07408.

930

Hrachowitz, M., Benettin, P., van Breukelen, B.M., Fovet, O., Howden, N.J.K., Ruiz, L., van der Velde, Y., Wade, A.J., 2016. Transit times – the link between hydrology and water quality at the catchment scale. WIREs Water 3, 629-657.

Kim, M., Boithias, L., Cho, K.H., Silvera, N., Thammahacksa, C., Latsachack, K., Rochelle-Newall, E., Sengtaheuanghoung, O., Pierret, A., Pachepsky, Y.A., Ribolzi, O., 2017. Hydrological modeling of Fecal Indicator Bacteria in a tropical mountain catchment. Water Research 119, 102-113.

Kinzelman, J.L., Singh, A., Ng, C., Pond, K.R., Bagley, R.C., Gradus, S., 2005. Use of IDEXX Colilert-18® and Quanti-Tray/2000 as a rapid and simple enumeration method for the implementation of recreational water monitoring and notification programs. Lake and Reservoir Management 21(1), 73-77.

Kirchner, J.W., 2006. Getting the right answers for the right reasons: Linking measurements, analyses, and models to advance the science of hydrology. Water Resources Research 42, W03S04.

Kirchner, J.W., Feng, X., Neal, C., Robson, A.J., 2004. The fine structure of water-quality dynamics: the (high-frequency) wave of the future. Hydrological Processes 18, 1353-1359.

Kling, H., Fuchs, M., Paulin, M., 2012. Runoff conditions in the upper Danube basin under an ensemble of climate change scenarios. Journal of Hydrology 424-425, 264–277.

Kundzewicz, Z.W., Mata, L.J., Arnell, N.W., Döll, P., Kabat, P., Jiménez, B., Miller, K.A., Oki, T., Sen, Z., Shiklomanov, I.A., 2007. Freshwater resources and their management: 173–210 in Parry, M., Canziani O., Palutikof, J., van der Linden, P., Hanson, C. (eds) Climate Change 2007: Impacts, Adaptation and Vulnerability. Contribution of Working Group II to the Fourth Assessment Report of the Intergovernmental Panel on Climate Change. Cambridge University Press: Cambridge, UK.

Kuppel, S., Tetzlaff, D., Maneta, M.P., Soulsby, C., 2018. EcH$_2$O-iso 1.0: Water isotopes and age tracking in a process-based, distributed ecohydrological model. Geoscientific Model Development Discussions, in review.

961 Langan, S.J., Wade, A.J., Smart, R.P., Edwards, A.C., Soulsby, C., Billett, M.F., Jarvie, H.P., Cresser, M.S.,
962 Owen, R., Ferrier, R.C., 1997. The prediction and management of water quality in a relatively unpolluted major
963 Scottish catchment: current issues and experimental approaches. Science of the Total Environment 194/195, 419-
964 435.
965
966 Lessels, J.S., Tetzlaff, D., Birkel, C., Dick, J., Soulsby, C., 2016. Water sources and mixing in riparian wetlands
967 revealed by tracers and geospatial analysis. Water Resources Research 52, 456-470.
968
969 McDonnell, J.J., Beven, K., 2014. Debates – The future of hydrological sciences: A (common) path forward? A
970 call to action aimed at understanding velocities, celerities and residence time distributions of the headwater
971 hydrograph. Water Resources Research 50, 5342-5350.
972
973 McDonnell, J.J., Sivapalan, M., Vaché, K., Dunn, S., Grant, G., Haggerty, R., Hinz, C., Hooper, R., Kirchner, J.,
974 Roderick, M.L., Selker, J., Weiler, M., 2007. Moving beyond heterogeneity and process complexity: A new vision
975 for watershed hydrology. Water Resources Research 43, W07301.
976
977 McMillan, H., Tetzlaff, D., Clark, M., Soulsby, C., 2012. Do time-variable tracers aid the evaluation of
978 hydrological model structure? A multimodel approach. Water Resources Research 48 W05501.
979
980 Mitchell, B., Staines, B.W., Welch, D., 1977. Ecology of Red Deer: A research review relevant to their
981 management in Scotland. Institute of Terrestrial Ecology, Cambridge.
982
983 Muirhead, R.W., Monaghan, R.M., 2012. A two reservoir model to predict *Escherichia coli* losses to water from
984 pastures grazed by dairy cows. Environmental International 40, 8-14.
985
986 Muirhead, R.W., Elliot, A.H., Monaghan, R.M., 2011. A model framework to assess the effect of dairy farms and
987 wild fowl on microbial water quality during base-flow. Water Research 45, 2863–2874.
988

Natvig, E. E., Ingham, S. C., Ingham, B. H., Cooperband, L. R., Roper, T. R., 2002. Salmonella enterica serovar Typhimurium and Escherichia coli contamination of root and leaf vegetables grown in soils with incorporated bovine manure. Applied and Environmental Microbiology 68(6), 2737-2744.

Oliver D.M., Clegg C.D., Haygarth P.M., Heathwaite A.L., 2005. Assessing the potential for pathogen transfer from grassland soils to surface waters. Advances in Agronomy 85, 125–180.

Oliver, D.M., Page, T., Heathwaite, A.L., Haygarth, P.M., 2010. Re-shaping models of E. coli population dynamics in livestock faeces: Increased bacterial risk to humans? Environmental International 36, 1-7.

Oliver, D.M., Porter, D.H., Heathwaite, A.L., Zhang, T., Quilliam, R.S., 2015. Impact of low intensity summer rainfall on *E. coli*-discharge event dynamics with reference to sample acquisition and storage. Environmental Monitoring and Assessment 187: 426.

Oliver, D.M., Porter, K.D.H., Pachepsky, Y.A., Muirhead, R.W., Reaney, S.M., Coeffey, R., Kay, D., Milledge, D.G., Hong, E., Anthony, S.G., Page, T., Bloodworth, J.W., Mellander, P., Carbonneau, P., McGrane, S.J., Quilliam, R.S., 2016. Predicting microbial water quality with models: Over-arching questions for managing risk in agricultural catchments. Science of the Total Environment 544, 39-47.

Page, T., Beven, K.J., Freer, J., Neal, C., 2007. Modelling the chloride signal at Plynlimon, Wales, using a modified dynamic TOPMODEL incorporating conservative chemical mixing (with uncertainty). Hydrological Processes 21, 292-307.

Porter, K.D.H., Reaney, S.M., Quilliam, R.S., Burgess, C., Oliver, D.M., 2017. Predicting diffuse microbial pollution risk across catchments: The performance of SCIMAP and recommendations for future development. Science of the Total Environment 609, 456-465.

Reaney, S.M., 2008. The use of agent based modelling techniques in hydrology: determining the spatial and temporal origin of channel flow in semi-arid catchments. Earth Surface Processes and Landforms 33, 317-327.

1019 Remondi, F., Kirchner, J.W., Burlando, P., Fatichi, S., 2018. Water flux tracking with a distributed hydrological
1020 model to quantify controls on spatio-temporal variability of transit time distributions. Water Resources Research
1021 54, WR021689.
1022
1023 Rodgers, P., Soulsby, C., Hunter, C., Petry, J., 2003. Spatial and temporal bacterial quality of a lowland
1024 agricultural stream in northeast Scotland. Science of the Total Environment 314-316, 289-302.
1025
1026 Sadeghi, A., Arnold, J., 2002. A SWAT/Microbial Sub-Model for Predicting Pathogen Loadings in Surface and
1027 Groundwater at Watershed and Basin Scales. In Total Maximum Daily Load (TMDL): Environmental
1028 Regulations, Proceedings of 2002 Conference (p. 56). American Society of Agricultural and Biological Engineers.
1029
1030 Seibert, J., Grabs, T., Koehler, S., Laudon, H., Winterdahl, M., Bishop, K., 2009. Linking soil- and stream-water
1031 chemistry based on riparian flow concentration integration model. Hydrological and Earth System Sciences 13,
1032 2287-2297.
1033
1034 Senjem, N., Ganske, L., Johnson, G., Morrison, D., Thompson, B., 2002. Regional Total Maximum Daily Load
1035 Evaluation of Fecal Coliform Bacteria Impairments In the Lower Mississippi River Basin in Minnesota. Retrieved
1036 from: https://www.pca.state.mn.us/sites/default/files/tmdl-final-lowermiss-fc02.pdf
1037
1038 Sivakumar, B., 2008. Dominant processes concept, model simplification and classification framework in
1039 catchment hydrology. Stochastic Environmental Research and Risk Assessment 22(6), 737-748.
1040
1041 SNH, 2016. Deer Management in Scotland: Report to the Scottish Government from Scottish National Heritage
1042 2016. Retrieved from: http://www.snh.org.uk/pdfs/publications/corporate/DeerManReview2016.pdf
1043
1044 Smith, A., Welch, C., Stadnyk, T., 2016. Assessment of a lumped coupled flow-isotope model in data scarce
1045 Boreal catchments. Hydrological Processes 30, 3871-3884.
1046

1047 Soulsby, C., Tetzlaff, D., Rodgers, P., Dunn, S., Waldron, S., 2006. Runoff processes, stream water residence
1048 times and controlling landscape characteristics in a mesoscale catchment: An initial evaluation. Journal of
1049 Hydrology 325, 197-221.
1050
1051 Soulsby, C., Birkel, C., Geris, J., Dick, J., Tunaley, C., Tetzlaff, D., 2015. Stream water age distributions
1052 controlled by storage dynamics and nonlinear hydrological connectivity: Modeling with high-resolution data.
1053 Water Resources Research 51.
1054
1055 Soulsby, C., Bradford, J., Dick, J., McNamara, J.P., Geris, J., Lessels, J., Blumstock, M., Tetzlaff, D., 2016. Using
1056 geophysical surveys to test tracer-based storage estimates in headwater catchments. Hydrological Processes 30,
1057 4434-4445.
1058
1059 Spence, C., Woo, M.K., 2003. Hydrology of subarctic Canadian Shield: soil-filled valleys. Journal of Hydrology
1060 279(1), 151-166.
1061
1062 Sprenger, M., Tetzlaff, D., Tunaley, C., Dick, J., Soulsby, C., 2017. Evaporation fractionation in a peatland
1063 drainage network affects stream water isotope composition. Water Resources Research 53, 851-866.
1064
1065 Stadler, P., Blöschl, G., Vogl, W., Koschelnik, J., Epp, M., Lackner, M., Oismüller, M., Kumpan, M., Nemeth,
1066 L., Strauss, P. and Sommer, R., Ryzinska-Paier, G., Farnleitner, A.H., Zessner., M., 2016. Real-time monitoring
1067 of beta-d-glucuronidase activity in sediment laden streams: A comparison of prototypes. Water research, 101,
1068 252-261.
1069
1070 Stadnyk, T.A., Delavau, C., Kouwen, N., Edwards, T.W.D., 2013. Towards hydrological model calibration and
1071 validation: simulation of stable water isotopes using the isoWATFLOOD model. Hydrological Processes 27,
1072 3791-3810.
1073
1074 Tetzlaff, D., Soulsby, C., Birkel, C., 2010. Hydrological connectivity and microbiological fluxes in montane
1075 catchments: the role of seasonality and climatic variability. Hydrological Processes 24, 1231-1235.
1076

1077 Tetzlaff, D., Birkel, C., Dick, J., Geris, J., Soulsby, C., 2014. Storage dynamics in hydropedological units control
1078 hillslope connectivity, runoff generation, and the evolution of catchment transit time distributions. Water
1079 Resources Research 50, 969-985.
1080
1081 Tetzlaff, D., Carey, S.K., McNamara, J.P., Laudon, H., Soulsby, C., 2017. The essential value of long-term
1082 experimental data for hydrology and water management. Water Resources Research 53, 2598-2604.
1083
1084 Tunaley, C., Tetzlaff, D., Birkel, C., Soulsby, C., 2017. Using high-resolution isotope data and alternative
1085 calibration strategies for a tracer-aided runoff model in a nested catchment. Hydrological Processes 31, 3962-
1086 3978.
1087
1088 Tunaley, C., Tetzlaff, D., Lessels, J., Soulsby, C., 2016. Linking high-frequency DOC dynamics to the ages of
1089 connected water sources. Water Resources Research 52, 5232-5247.
1090
1091 Tyrrel, S.F., Quinton, J.N., 2003. Overland flow transport of pathogens from agricultural land receiving faecal
1092 wastes. Journal of Applied Microbiology 94, 87S-93S.
1093
1094 Vaché, K.B., McDonnell, J.J., 2006. A process-based rejectionist framework for evaluating catchment runoff
1095 model structure. Water Resources Research 42, W02409.
1096
1097 van Huijgevoort, M.H.J., Tetzlaff, D., Sutanudjaja, E.H., Soulsby, C., 2016. Using high resolution tracer data to
1098 constrain water storage, flux and age estimates in a spatially distributed rainfall-runoff model. Hydrological
1099 Processes 30, 4761-4778.
1100
1101 Wells, C., Ketcheson, S., Price, J., 2017. Hydrology of a wetland-dominated headwater basin in the Boreal Plain,
1102 Alberta, Canada. Journal of Hydrology 547, 168-183.
1103
1104 Westerberg, I.K., Birkel, C., 2015. Observational uncertainties in hypothesis testing: investigating the
1105 hydrological functioning of a tropical catchment. Hydrological Processes 29, 4863-4879.
1106

1107 Whitehead, P.G., Leckie, H., Rankinen, K., Butterfield, D., Futter, M.N., Bussi, G., 2016. An INCA model for
1108 pathogens in rivers and catchments: Model structure, sensitivity analysis and application to the River Thames
1109 catchment, UK. Science of the Total Environment 572, 1601-1610.
1110
1111 Wilkinson, R.J., McKergow, L.A., Davies-Colley, R.J., Ballantine, D.J., Young, R.G., 2011. Modelling storm-
1112 event *E. coli* pulses from the Motueka and Sherry Rivers in the South Island, New Zealand. New Zealand Journal
1113 of Marine and Freshwater Research 45(3), 369-393.
1114
1115 Zhang, Z., Chen, X., Soulsby, C., 2017. Catchment-scale conceptual modelling of water and solute transport in
1116 the dual flow system of the karst critical zone. Hydrological Processes 31, 3421-3436.
1117
1118 Zhang, Z., Chen, X., Soulsby, C., Cheng, Q., 2018. Storage dynamics, hydrological connectivity and flux ages in
1119 a karst catchment: conceptual modelling using stable isotopes. Hydrological and Earth Systems Sciences
1120 Discussion, Accepted for Publication.

1121 Figure 1: The Bruntland Burn catchment showing a) Topography, extent of dynamic saturated riparian
1122 zone and location of stream monitoring; b) Main soil classes.

1123
1124

1125 Figure 2: Conceptual diagrams of: a) The tracer-aided hydrological model. Variables in red are model
1126 inputs (P = precipitation; PET = potential evapotranspiration; dSat = daily saturation extent); black
1127 represents hydrological dynamic storage (S_{up}, S_{sat}, S_{low}) and processes (flux equations for Q_{up}, Q_{sat}, Q_{low}
1128 and R, AET = actual evapotranspiration); green relates to isotope tracer simulation (c = isotopic
1129 composition, $frac_{sat}$ = fractionation in riparian zone, MV = mixing volume); blue are parameters to be
1130 calibrated (a, b, r, k, α = rate parameters, α_{ET} = isotopic depletion factor; upS_p, $satS_p$, $lowS_p$ = mixing
1131 volumes). b) The faecal coliform (FC) model. Purple variables are defined randomly at each time-step
1132 (Deer In Catchment = binary variable to determine if deer are present or not, Total Deer = total number
1133 of deer in catchment if present, Excretion = load of FC excreted per deer per day). For the hillslope (up)

and riparian zone (sat), the variables deer, FCProd, FC, dieOff and FC_Flux are: number of deer in source area as determined by the seasonal probability function, FC load added to storage, FC storage, die-off from storage (calculated using Eq. 3), and FC Flux from hillslope to riparian zone and riparian zone to the stream. Q_{up} and Q_{sat} are simulated runoff from the dynamic hillslope and dynamic riparian zone, and $maxQ_{obs}$ is the maximum observed discharge for the study period. The "min" function is used in calculating FC fluxes to ensure that FC is not created if the model simulates runoff that exceeds the maximum observed discharge.

Figure 3: Time series of a) Precipitation and stream discharge; b) Air temperature and potential evapotranspiration (PET); c) Isotopic composition of stream water and precipitation (symbol sizes proportional to precipitation amount); d) Stream faecal coliform (FC) concentrations (Conc.) and loads – concentrations below the limit of detection (LOD) are plotted in red at the LOD (1 CFU $100ml^{-1}$), with the upper limits of associated loads calculated using the LOD as the concentration.

Figure 4: Time series of a) Precipitation, and of median simulated model outputs for b) Stream discharge, groundwater and instantaneous contributions of the hillslope and riparian zone to water available for evapotranspiration and runoff generation from the riparian zone; c) Stream faecal coliform (FC) load and instantaneous contributions of the hillslope and riparian zone to FC available for mobilisation from the riparian zone; d) Total FC stored in the catchment and distribution between the hillslope and riparian zone at the end of a given timestep.

Figure 5: Time series of a) Observed and modelled stream discharge; b) Observed and modelled stream water isotopic composition; c) Observed and modelled stream faecal coliform (FC) loads. When an observed concentration (conc.) was below the limit of detection (LOD), an upper limit for the associated FC load (+) was calculated using 1 CFU 100 ml^{-1} as the concentration. $Log_{10}(0)$ indicates periods when loads of FC were simulated to be 0 CFU day^{-1}. The blue shaded area in c) indicates the period potentially impacted by freeze-thaw cycles.

Tables

Table 1: Initial and calibrated ranges for the hydrological and isotope parameters of the model. Initial ranges for all parameters were informed by Birkel et al. (2010; 2015), with the exception of α_{ET} taken from Benettin et al. (2017).

Parameter	Units	Initial Range	Calibrated Range Median [5th percentile, 95th percentile]
Hydrology			
a	day^{-1}	[0.2, 0.8]	0.48 [0.23, 0.76]
b	day^{-1}	[0.0001, 0.1]	0.036 [0.0028, 0.088]
r	day^{-1}	[0.2, 0.9]	0.60 [0.28, 0.87]
k	day^{-1}	[0.001, 0.1]	0.053 [0.014, 0.095]
α	-	[0.1, 0.9]	0.55 [0.27, 0.85]
Isotopes			
upS_p	mm	[0, 1000]	363 [136, 721]
$satS_p$	mm	[0, 1000]	88 [12, 237]
$lowS_p$	mm	[0, 1000]	534 [64, 952]

α_{ET}	-	[0.95, 1.0]	0.97 [0.95, 0.99]

Declarations of Interest: None

Author Contributions: AJN adapted a tracer-aided hydrological model developed in earlier work led by DT and CS, and coupled this to a faecal coliform model written by AJN with input from all co-authors. Data collection for use in model calibration was led by DT and CS. All authors were involved in data and model interpretation. AJN prepared the manuscript with contributions from all co-authors. All authors have approved the final manuscript.

Highlights

- Couple faecal coliform (FC) and tracer-aided models to explore drivers of FC loads
- Good simulation of discharge and isotopes indicates hydrological process realism
- Connectivity sustains stores of FC available for transfer to the stream in summer
- Freeze-thaw cycles or a hillslope connectivity dilution effect may be key in winter
- Spatially-distributed models and enhanced FIO data collection are useful next steps

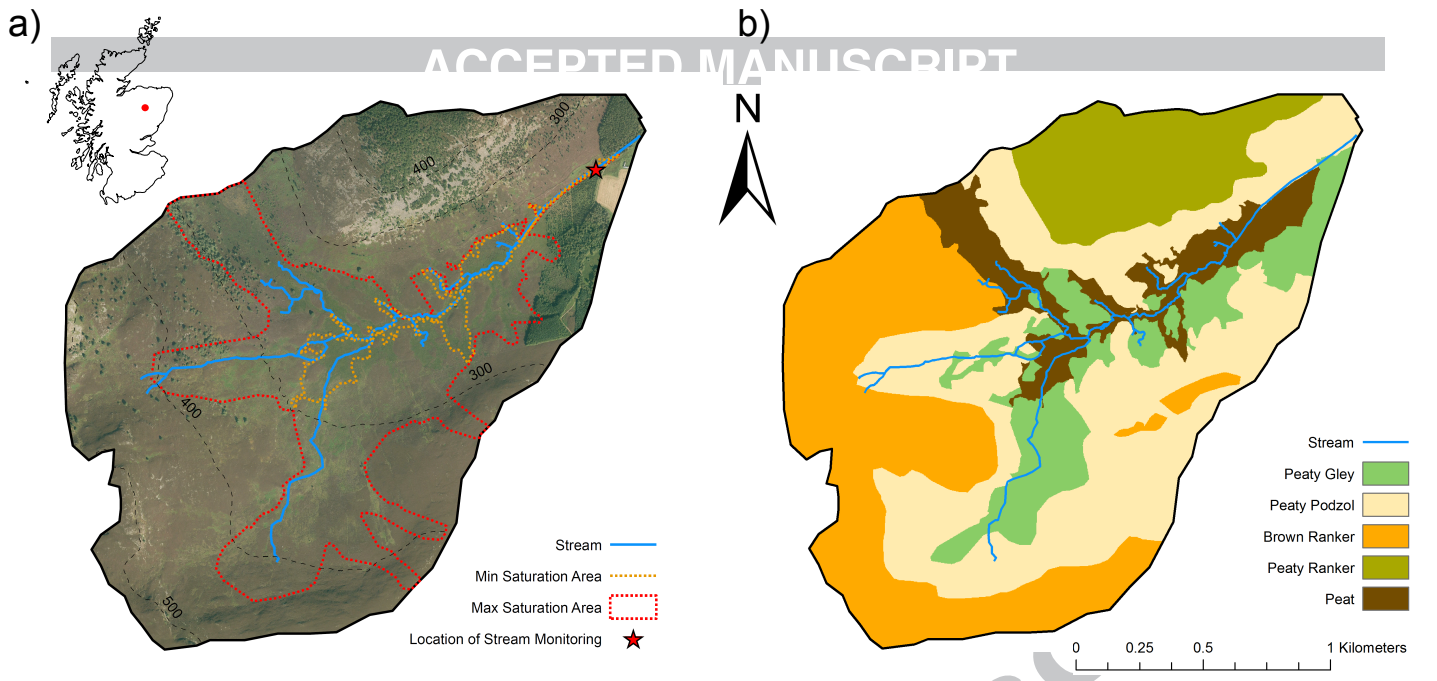

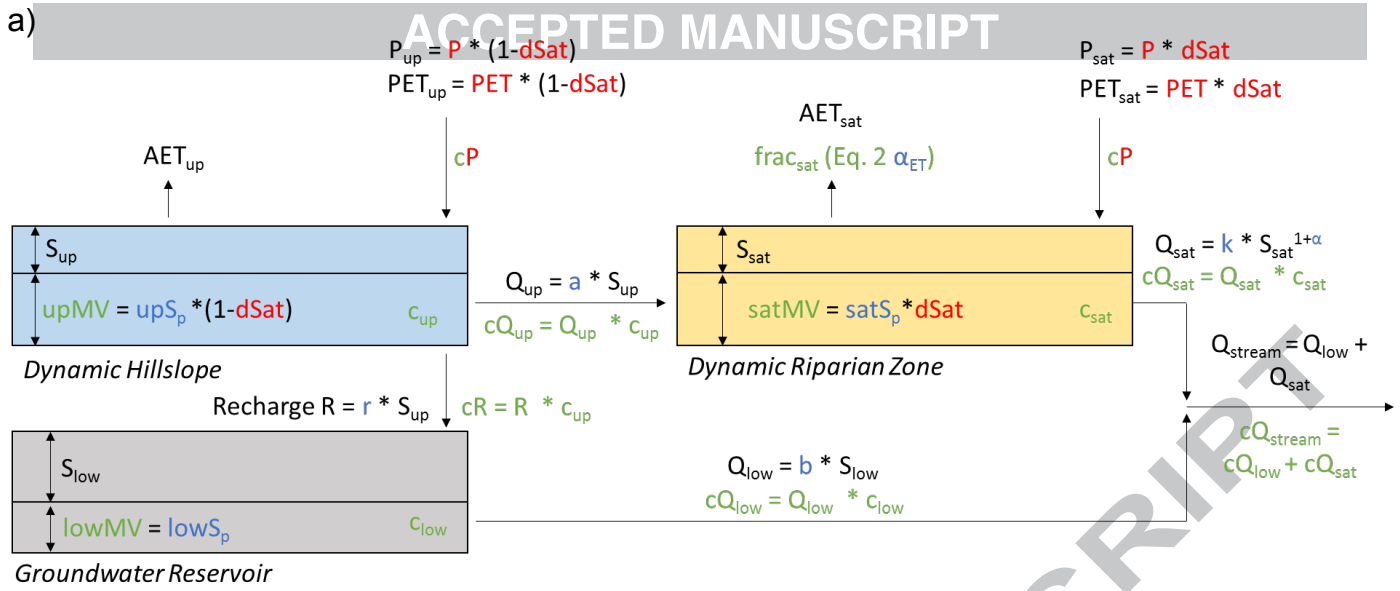

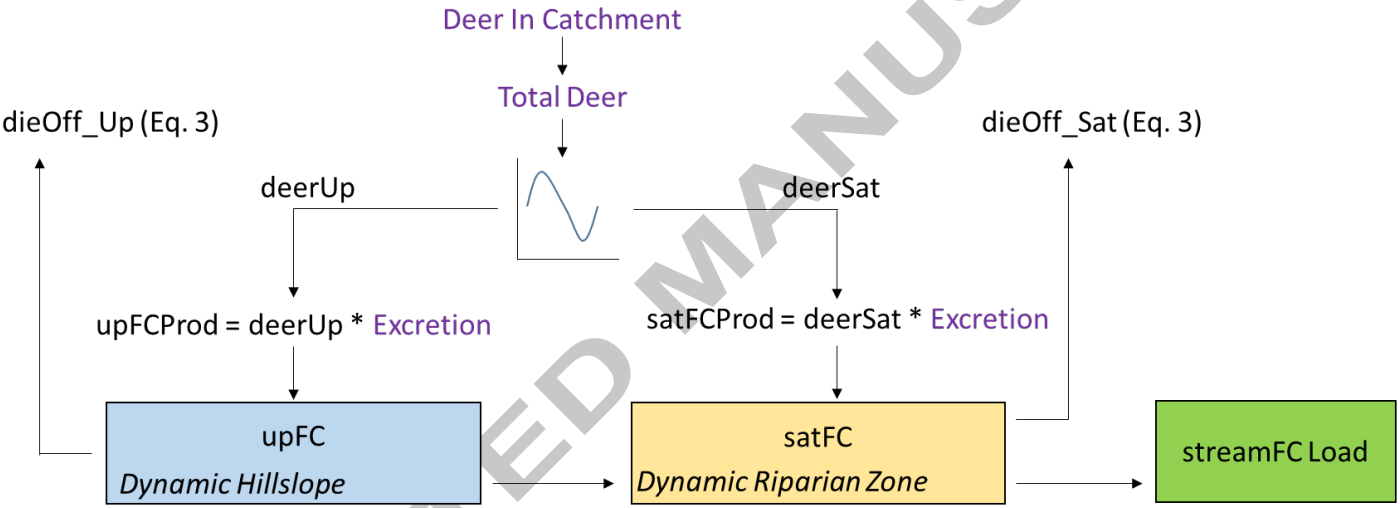

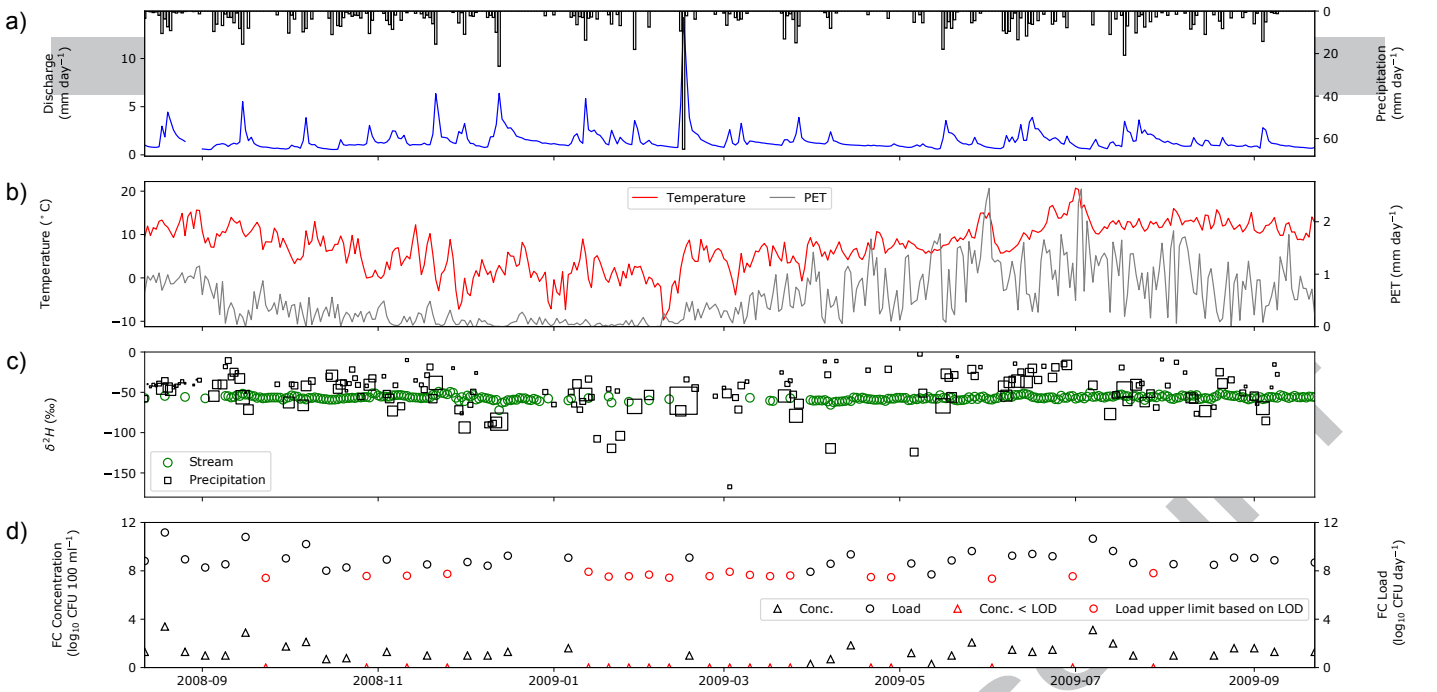
a)
Discharge (mm day⁻¹)
Precipitation (mm day⁻¹)
b)
Temperature (° C)
Temperature
PET
PET (mm day⁻¹)
c)
δ²H (‰)
Stream
Precipitation
d)
FC Concentration (log10 CFU 100 ml⁻¹)
Conc.
Load
Conc. < LOD
Load upper limit based on LOD
FC Load (log10 CFU day⁻¹)
2008-09
2008-11
2009-01
2009-03
2009-05
2009-07
2009-09

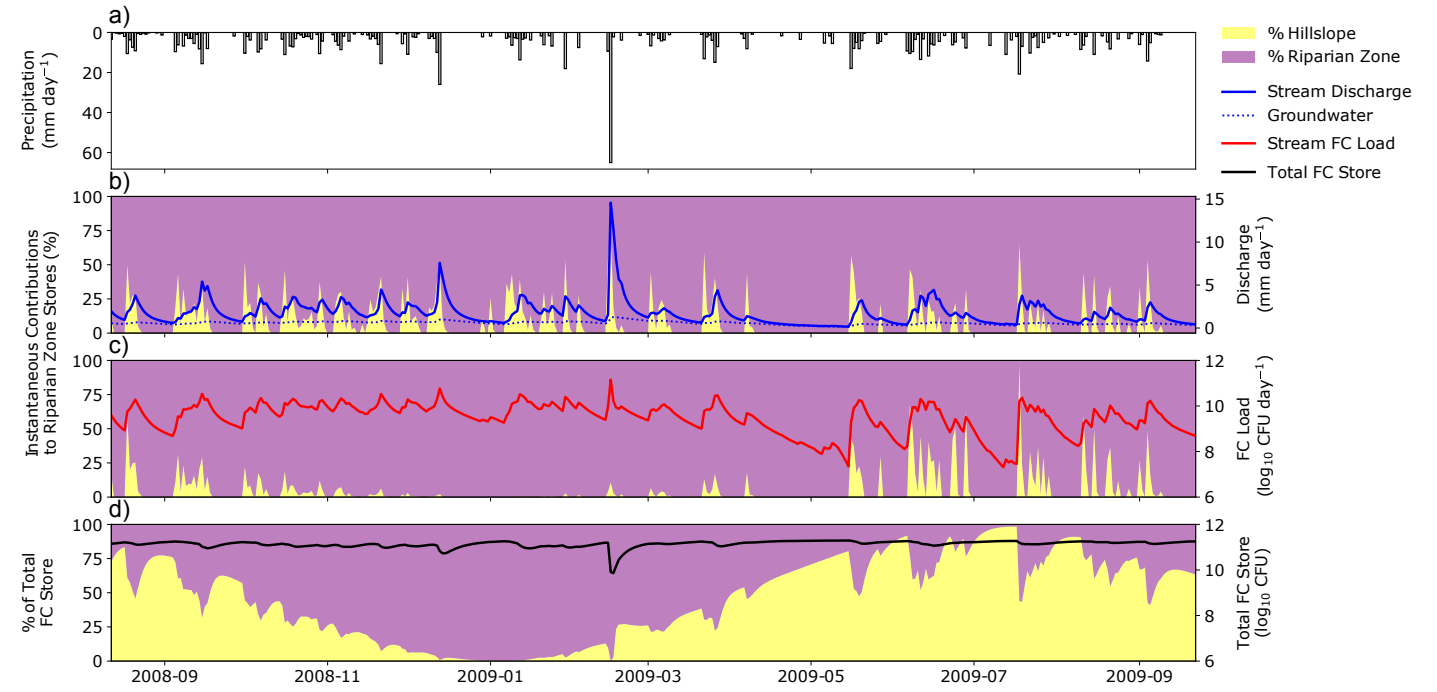
a)
b)
c)
d)
Precipitation (mm day⁻¹)
Instantaneous Contributions to Riparian Zone Stores (%)
Discharge (mm day⁻¹)
FC Load (log10 CFU day⁻¹)
% of Total FC Store
Total FC Store (log10 CFU)
% Hillslope
% Riparian Zone
Stream Discharge
Groundwater
Stream FC Load
Total FC Store
2008-09
2008-11
2009-01
2009-03
2009-05
2009-07
2009-09

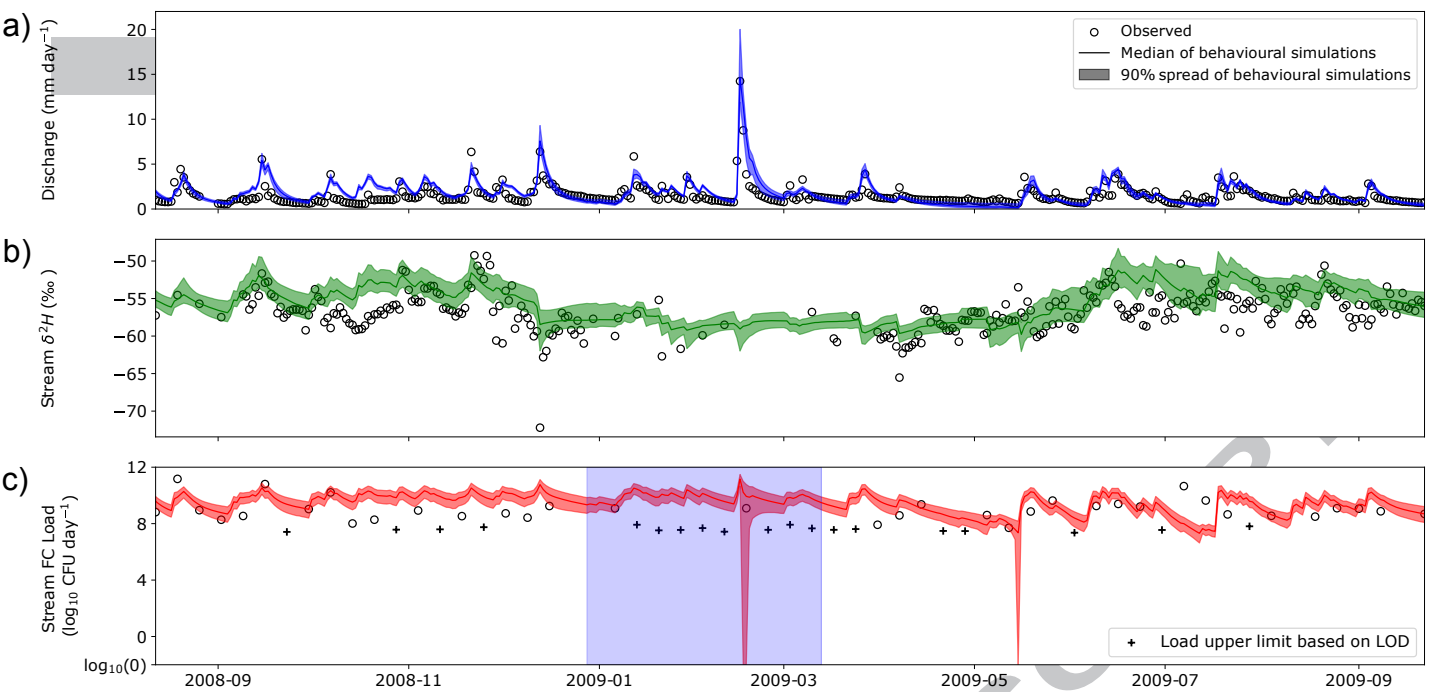
a)
Discharge (mm day^{-1})
20
15
10
5
0
Observed
Median of behavioural simulations
90% spread of behavioural simulations
b)
Stream δ^2H (‰)
−50
−55
−60
−65
−70
c)
Stream FC Load
($\log_{10}$ CFU day^{-1})
12
8
4
0
$\log_{10}(0)$
Load upper limit based on LOD
2008-09
2008-11
2009-01
2009-03
2009-05
2009-07
2009-09